The impact of ultra-high field MRI on cognitive and computational neuroimaging

NeuroImage 168 (2018) 366–382

Contents lists available at ScienceDirect

NeuroImage

journal homepage: www.elsevier.com/locate/neuroimage

The impact of ultra-high field MRI on cognitive and computational neuroimaging

Federico De Martino[a,b,1,*], Essa Yacoub[b,1], Valentin Kemper[a], Michelle Moerel[a,c], Kâmil Uludağ[a], Peter De Weerd[a], Kamil Ugurbil[b], Rainer Goebel[a], Elia Formisano[a,c]

[a] Department of Cognitive Neurosciences, Faculty of Psychology and Neuroscience, Maastricht University, Oxfordlaan 55, 6229 ER Maastricht, The Netherlands
[b] Center for Magnetic Resonance Research, Department of Radiology, University of Minnesota, 2021 sixth street SE, 55455 Minneapolis, MN, USA
[c] Maastricht Center for System Biology, Maastricht University, Universiteitssingel 60, 6229 ER Maastricht, The Netherlands

ARTICLE INFO

Keywords:
Ultra high magnetic fields
High spatial resolution
Subcortical
Computational models
Cortical laminae
Cortical columns

ABSTRACT

The ability to measure functional brain responses non-invasively with ultra high field MRI (7 T and above) represents a unique opportunity in advancing our understanding of the human brain. Compared to lower fields (3 T and below), ultra high field MRI has an increased sensitivity, which can be used to acquire functional images with greater spatial resolution, and greater specificity of the blood oxygen level dependent (BOLD) signal to the underlying neuronal responses.

Together, increased resolution and specificity enable investigating brain functions at a submillimeter scale, which so far could only be done with invasive techniques. At this *mesoscopic* spatial scale, perception, cognition and behavior can be probed at the level of fundamental units of neural computations, such as cortical columns, cortical layers, and subcortical nuclei. This represents a unique and distinctive advantage that differentiates ultra high from lower field imaging and that can foster a tighter link between fMRI and computational modeling of neural networks.

So far, functional brain mapping at submillimeter scale has focused on the processing of sensory information and on well-known systems for which extensive information is available from invasive recordings in animals. It remains an open challenge to extend this methodology to uniquely human functions and, more generally, to systems for which animal models may be problematic. To succeed, the possibility to acquire high-resolution functional data with large spatial coverage, the availability of computational models of neural processing as well as accurate biophysical modeling of neurovascular coupling at *mesoscopic* scale all appear necessary.

Introduction

Since its introduction (Bandettini et al., 1992; Kwong et al., 1992; Ogawa et al., 1992), functional magnetic resonance imaging (fMRI) has taken the field of cognitive neuroscience by storm. Here we aim at highlighting the potential for imaging brain function at ultra high fields (UHF, 7 T and above). In more than twenty years of fMRI research, our understanding of the complex physiological changes that underlie the fMRI signal (i.e. the neurovascular coupling and the hemodynamic response (Uludag et al., 2009)) has considerably advanced. As a result, the confidence in interpreting the fMRI signal has increased and fMRI has become the method of choice for many studies of basic sensory processing (e.g. visual, auditory and somatosensory) and higher cognitive functions (e.g. memory, language, emotions) (see Fig. 1). Other factors contributing to the ever increasing number of fMRI applications have been the ability to map human brain function at a high spatial resolution non-invasively with large spatial coverage and the availability of research dedicated MRI scanners. Using fMRI (at a spatial resolution of 8 mm^3 or lower) it has been possible to investigate preferential responses of cortical areas for specific stimulus categories (Belin et al., 2000; Kanwisher et al., 1997) and the coarse large-scale topographic representation of sensory features (Sereno et al., 1995).

As a result of continuous technical advances (Moeller et al., 2010; Setsompop et al., 2012; Xu et al., 2013), functional imaging at conventional field strengths (≤3 T) can now be performed at a resolution of 8 mm^3 (a threefold improvement compared to early fMRI studies) with sub-second temporal resolution (see e.g. protocols at http://www.humanconnectome.org/) (Ugurbil et al., 2013). In spite

* Correspondence to: Department of Cognitive Neurosciences, Faculty of Psychology, University of Maastricht, Postbus 616, 6200 MD Maastricht, The Netherlands.
E-mail address: f.demartino@maastrichtuniversity.nl (F. De Martino).
[1] Equal contribution.

http://dx.doi.org/10.1016/j.neuroimage.2017.03.060
Received 20 October 2016; Accepted 29 March 2017
Available online 08 April 2017
1053-8119/

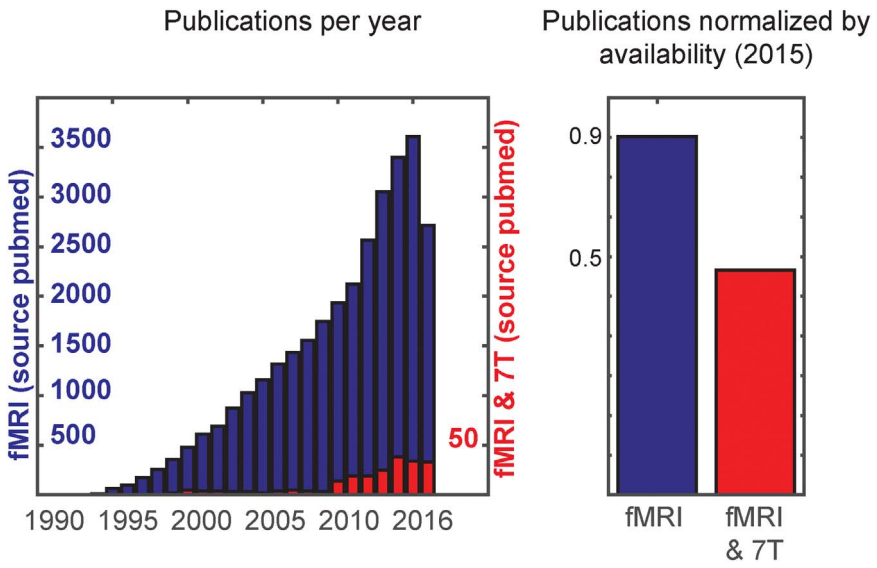

Fig. 1. (Left) Number of publications (source Pubmed) that result from a search including the terms "fMRI" (blue) or "fMRI and 7 T" (red). (Right) Number of publications (source Pubmed) for the year 2015 ("fMRI" (blue) or "fMRI and 7 T" (red)) normalized by the number of available scanners estimated to be 20000 3 T and 1.5 T scanners (of which only 4000 are actually available for research) and 60 7 T scanners.

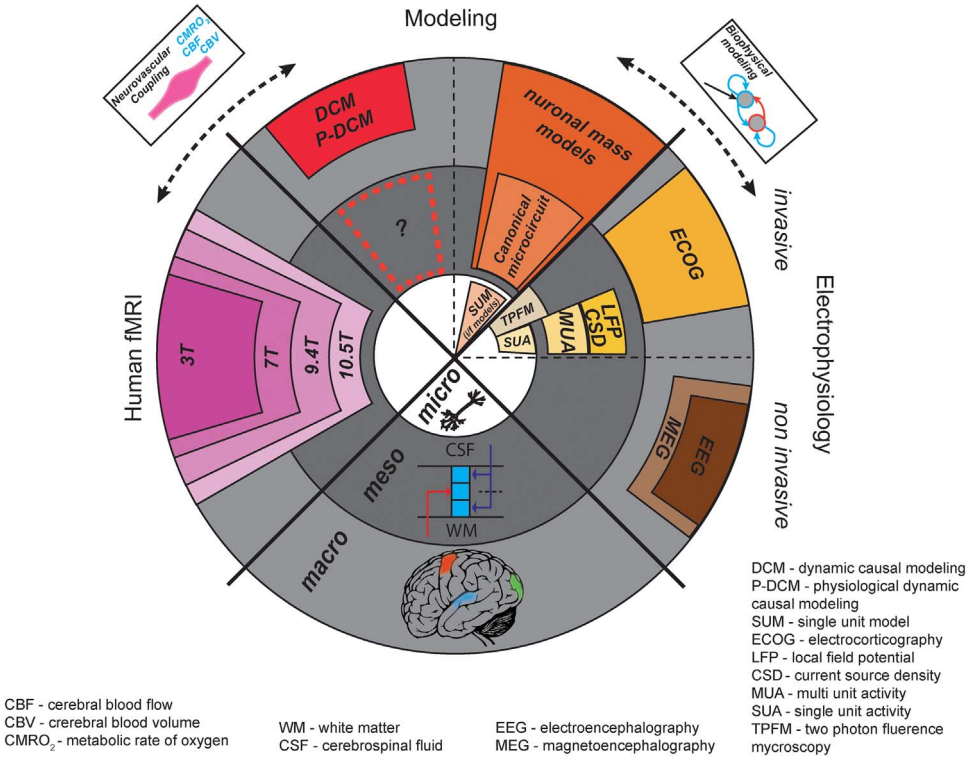

Fig. 2. Comparing field dependent human fMRI with electrophysiology and computational modeling of neural networks. The radius represents the spatial scale of the investigation (micro [< 0.001 mm^3], meso [< =1 mm^3] and macro [> 10 mm^3]). At field strength of 7 T and higher measuring functional responses at both the macroscopic and mesoscopic scale is possible. Generative models of the neurovascular coupling at the macrospopic scale (e.g. DCM) allow linking non-invasive macroscopic data with neuronal mass models and with non-invasive and invasive electrophysiological data. Biophysical modeling is required to bridge computational models at different spatial scales (e.g. neural mass models, canonical microcircuit) with invasive and non-invasive electrophysiological measures.

of these advances, the spatial resolution of fMRI at conventional field strengths still poses limitations on the study of the human brain. Inspired by histological studies (y Cajal, 1995), invasive electrophysiology has shown that the cortex is organized in distinct cortical layers with unique functional properties (e.g. feed-forward processing and feedback processing) and that cortical areas are composed of processing units that share preference for one stimulus feature across the cortical depth (i.e. cortical columns) (Hubel and Wiesel, 1968; Mountcastle, 1997). The role of subcortical structures and their subdivisions in both feed-forward and feedback processing has also been extensively investigated (e.g. the role of the inferior colliculus in processing sound information; (FitzPatrick, 1975; Merzenich and Reid, 1974; Winer and Schreiner, 2005). The plethora of information coming from invasive research suggest that the *mesoscopic* organizational level of the brain represents an intermediate comprehensive level of analysis, at which information from single neurons (*microscopic* scale) and large-scale areal function (*macroscopic* scale) meet (Mitra, 2014) (Fig. 2).

The continuous development of fMRI techniques has been paralleled by the development of analysis strategies. Functional responses have been analyzed to link behavioral, cognitive and perceptual changes to the measured fMRI signals by investigating differences between experimental conditions in single voxels (i.e. the General Linear Model [GLM]) (Friston et al., 1995) or by considering the information in spatial patterns of responses (i.e. multivoxel pattern analysis [MVPA], fMRI-decoding, representational similarity analysis [RSA]) (Cox and Savoy, 2003; De Martino et al., 2008; Formisano et al., 2008; Haxby et al., 2001; Kriegeskorte et al., 2008; Pereira et al., 2009; Staeren et al., 2009) and in functionally connected brain networks (Greicius et al., 2003). More recently, several analysis techniques (population receptive field [pRF] mapping, fMRI encoding and model based decoding) (Dumoulin and Wandell, 2008; Kay et al., 2008; Naselaris et al., 2010; Wandell, 1999; Wandell and Winawer, 2015) have been introduced in order to link fMRI signals with computational models of brain function.

Analysis techniques such as MVPA or RSA have been proposed to leverage the mesoscopic scale information distributed over multiple large (> 1 mm isotropic) voxels (Haynes and Rees, 2005; Kamitani and Tong, 2005). However, the source of this information remains uncertain (see section on "Analyzing patterns of fMRI responses: MVPA and RSA" for more details). At conventional field strengths, only a few studies (Koopmans et al., 2010; Ress et al., 2007) have attempted mapping (i.e. spatially localize) non-invasively the human brain at the mesoscopic scale (Fig. 2).

In other words, linking computations of single columns and layers to imaging data collected *in vivo* is a task that necessitates high spatio-temporal resolution with sufficient temporal signal to noise ratio (tSNR), which is typically not available at conventional field strengths. Similar limitations apply when imaging functional properties within small subcortical structures and the cerebellum. For technical reasons (e.g. the properties and geometry of receive coils), the sensitivity of fMRI is higher in the cortex of the human brain compared to the thalamus or the brainstem. This poses additional constraints when imaging subcortical structures for which high resolution is essential given their small size.

Increasing field strength is accompanied by increases in the image signal to noise ratio (SNR) (Pohmann et al., 2016; Ugurbil et al., 2003; Vaughan et al., 2001) and in the BOLD contrast. In turn these can be traded for increasing the spatial resolution, up to 0.7 mm^3 (e.g. 0.9 mm isotropic) in a large field of view (Vu et al., 2016a) or even 0.27 mm^3 in a small visual region (Heidemann et al., 2012). Together with this increase in functional SNR, modeling studies have shown that higher magnetic fields are additionally advantageous as the BOLD signal becomes more sensitive to the microvasculature (Uludag et al., 2009) and in turn more accurate with respect to the site of neuronal activity. The increased SNR does not necessarily translate to an increased tSNR, the relation between these two is dependent on the impact of physiological and thermal noise (Triantafyllou et al., 2005). In low SNR regimes (e.g. as when acquiring high spatial resolution functional images), thermal noise dominates and increasing SNR results in increased tSNR. In high SNR regimes dominates (e.g. moderate to low spatial resolution acquisitions), physiological noise dominates and correction strategies to limit the impact of this source of noise have to be considered (Hutton et al., 2011).

The high SNR available at UHF enables alternative imaging strategies (i.e. non BOLD based measures) such as cerebral blood volume (CBV) based fMRI (Lu et al., 2003). It has been proposed that CBV-based fMRI is more specific to the underlying neuronal activation in comparison to gradient echo (GE)- based BOLD fMRI (Zhao et al., 2005, 2006) and initial promising results for non invasive measurements in humans have been reported (Guidi et al., 2016; Huber et al., 2015, 2016) (for a review see (Lu and van Zijl, 2012)).

In the last few years, recognition of the advantages of UHF has promoted a gradual shift to imaging the brain at field strengths higher than 3 T (see Fig. 1 and (van der Zwaag et al., 2016)). However, despite the efforts in several research groups, functional imaging at UHF remains a niche. Of course, the availability of UHF MR scanners is a major limiting factor. But normalizing the number of publications by the number of available scanners does not account completely for the differences observed between the numbers of studies conducted at 3 T and at 7 T (see Fig. 1). Thus, the open technical challenges of UHF and, especially, the availability of instruments that provide easy-to-use solutions to these technical challenges appear to be still factors limiting the transition to higher field (≥7 T) scanners for human cognitive neuroscience investigations. As UHF scanner availability is increasing and new developments are steadily mitigating the open technical challenges, the field of cognitive neuroscience is likely ready for a definitive paradigm shift.

Many reviews have presented discussed the advantages and disadvantages of different imaging strategies at UHF (see e.g. (Turner, 2016; Ugurbil, 2016; van der Zwaag et al., 2016)). Here we tie methodological considerations on analysis techniques such as univariate statistical modeling, MVPA, RSA and computational modeling to UHF imaging. We present concrete examples that we draw from the study of the (computational) processes underlying the perception of sounds (and its modulation by cognitive demands). Finally, we offer an overview on the current state of functional imaging at UHF by reviewing applications to higher cognitive functions in the study of both cortical and subcortical processing and try to outline the current limits in the interpretability of UHF fMRI data.

Imaging functional responses in vivo

The nature of BOLD fMRI

Since its introduction, a main criticism of fMRI has been its indirect link to neuronal activity (Logothetis, 2008; Ugurbil, 2016; Uğurbil et al., 2003). Signals measured by fMRI reflect vascular and metabolic consequences of neuronal activity and their accuracy with respect to the neuronal processes of interest (i.e. specificity) is strongly dependent on the way that these vascular/metabolic changes are measured. As such, the spatial specificity of fMRI signals depends on both physiology and MRI physics. To contextualize our review of analysis methods and applications, we discuss below the main issues (e.g. neuronal specificity and signal sensitivity) related with measuring fMRI signals and their dependence with field strength. For a more in depth account of the vascular origins of the fMRI signal and its implications for UHF fMRI we refer to (Uludag and Binder, 2017). in this same special issue.

The majority of in vivo human fMRI research measures physiological changes through the BOLD signal (Ogawa et al., 1990), which reflects the changes in concentration of deoxyhemoglobin (dHb) due to changes in oxygen consumption ($CMRO_2$), cerebral blood flow (CBF) and cerebral blood volume (CBV) both within (*intravascular*) and around (*extravascular*) vessels. Seminal investigations with simultaneous recordings of fMRI signals and electrophysiology have demonstrated the link between fMRI signal changes and synaptic activity reflected in the local field potentials (LFPs) (Logothetis et al., 2001). More generally, the BOLD fMRI signal in a voxel has been shown to reflect changes in the excitatory-inhibitory (EI) balance of a large population of neurons within that voxel (Logothetis, 2008). However, changes in dHb associated with neuronal activity happen both locally and in large distant veins that drain blood from the original activation site (Boxerman et al., 1995; Frahm et al., 1994; Gati et al., 1997; Lai et al., 1993; Turner, 2002; Yacoub et al., 2005). Thus, the BOLD fMRI signal measured in a voxel reflects *local* (i.e. within a voxel) changes in EI balance only to the extent that the distant effects can be ruled out.

The mainstream method of imaging BOLD changes uses a gradient-recalled echo (GE) signal to generate the contrast (T_2* weighting) in combination with echo planar imaging (EPI) (Mansfield, 1977) to acquire the data. This technique is sensitive to both *intra- and*

extravascular changes in dHb, originating from small to large diameter vessels (Boxerman et al., 1995; Uludag et al., 2009). As such, spatially distant effects from within and around larger vessels affect GE-EPI images. To reduce this effect, spin echo (SE) based BOLD images at UHF can be acquired. The main advantage of SE based contrast is that the *extravascular* contribution to the signal is weighted towards changes happening around small diameter vessels (Boxerman et al., 1995; Uludag et al., 2009) or dynamic averaging effects (T_2 contrast). This happens due to the refocusing of static averaging effects (T2') and the consequent suppression of the extravascular effects contributing to functional mapping signals originating from large diameter veins. Further, while the *intravascular* contribution from large vessels to the SE signal dominates at lower fields, the amount of *intravascular* weighting is inversely proportional to the field strength, and significantly reduced at field strengths higher than 7 T and higher at typical echo times employed for SE functional imaging (see below) (Uludag et al., 2009).

Signal changes with field strength and sequences

Moving to higher magnetic fields has two fundamental benefits. First, the signal to noise ratio (SNR) increases at least linearly with field strength (Vaughan et al., 2001) and, second, the BOLD contrast itself increases more than linearly with field (Ugurbil, 2016; Ugurbil et al., 2003). As a consequence, the functional contrast to noise ratio increases substantially with field strength. This benefits imaging brain regions (e.g. subcortical areas) that at conventional fields are characterized by insufficient SNR or experimental paradigms that are starved by sensitivity. The increase in functional contrast to noise can also be used to increase imaging resolution and benefits imaging techniques (e.g. SE imaging or CBV imaging) that are characterized by low sensitivity.

As stated above, the *intravascular* contribution to the GE and SE BOLD signal is reduced at ultra high magnetic fields (≥7 T) (Uludag and Binder, 2017; Uludag et al., 2009). *Intravascular* signals are a source of unspecific responses, as they are in part generated by large draining veins. These large veins often show a different specificity, or no specificity at all, compared to the underlying gray matter tissue (Budde et al., 2014; Goense and Logothetis, 2006; Yacoub et al., 2007, 2005). The reduced *intravascular* contribution makes both GE and SE more weighted towards extravascular signal contributions at UHF compared to conventional field strengths (3 T and below). What distinguishes GE and SE BOLD signals, and their respective spatial specificities, at UHF is thus the origin of their *extravascular* sensitivities. Extravascular signals around smaller vessels increase with the square of the magnetic field, while the signal around larger vessels increases more linearly. In SE imaging, the effect around larger vessels tends to be refocused, while in GE imaging this effect persists. Consequently, despite the overall higher sensitivity to smaller diameter vessels at higher fields, the GE signal at UHF is still significantly affected by large diameter vessels, which are sources of unspecific signals. For this reason, laminar investigations that have employed GE-EPI have shown an overall increase in functional contrast towards the cortical surface (De Martino et al., 2013b; Huber et al., 2015; Koopmans et al., 2010, 2011; Polimeni et al., 2010; Siero et al., 2011).

Recent modeling efforts have shown that the laminar spread of GE BOLD signals can be partly explained by taking into account the cortical vasculature and draining effects (Markuerkiaga et al., 2016) or by coupling the hemodynamic effect across layers (Heinzle et al., 2016). In practice, dealing with this potential source of non-specific responses is not trivial. One proposal has been to filter out signals from large vessels (i.e. the pial surface where the large draining veins are located, (Ahveninen et al., 2016; Barth and Norris, 2007; Chen et al., 2013; Fracasso et al., 2014; Nasr et al., 2016; Polimeni et al., 2010; Yu et al., 2012)). It is unclear to what extent this approach is safe from the effects that can still be measured at a distance away (the extravascular effect) from the large vessels. Further, in the absence of accurate methods to image the vasculature in vivo, the influence of large penetrating radial vessels to the measured data is even harder to evaluate. These penetrating vessels reduce laminar sensitivity and may mimic columnar-like neuronal activity.

T_2 (or SE) weighted acquisitions, on the other hand, benefit from the increased SNR and the reduced *intravascular* signal available at higher fields, providing an option to more accurately measure functional responses (Yacoub et al., 2003, 2005), albeit at the expense of lower magnitude of the BOLD contrast (i.e. the magnitude of the signal change associated with alteration in neuronal activity) compared to GE methods. The increased specificity has pushed developments for whole brain SE type of acquisitions at UHF (Boyacioglu et al., 2014; Hua et al., 2014; Koopmans et al., 2012; Scheffler and Ehses, 2016). Achieving purely T2 (SE) weighted acquisitions at UHF is extremely inefficient and power hungry, which is not practical for most high-resolution fMRI applications with large coverage. Additionally, when used in combination with EPI, some GE (T_2*) contrast is introduced, depending on the EPI readout times (Goense and Logothetis, 2006), which become necessarily long relative to the local T_2* (see e.g. (Kemper et al., 2015) for an evaluation of the impact of the readout train length on SE-EPI applied to laminar fMRI in humans at 7 T). To limit the non-specific effects caused by long EPI readouts segmented EPI acquisitions or sequences with reduced fields of view (e.g. 3D-GRASE with inner volume selection, (Oshio and Feinberg, 1991)) can be used (see e.g. (Kemper et al., 2015, 2016)). The necessity to limit the duration of the EPI readout trains means efficient high-resolution SE images for fMRI comes at the expense of volume coverage. Consequently, high-resolution SE fMRI at UHF requires additional considerations when setting up experimental designs (e.g. longer sessions, more stimulus repetitions, favoring powerful presentations schemes such as block designs or fast event related design).

Interpreting BOLD signal changes

In conclusion, while the link between fMRI signals and neuronal activity is well established, its interpretation is dependent on a variety of factors. Some of them are field independent as they also affect other hemodynamic–based methods, such as intrinsic optical imaging, and deal mostly with the neurovascular coupling. In addition, when using BOLD based functional contrast, similar signal changes (i.e. positive or negative BOLD responses) can be obtained from both changes in neuronal excitation and inhibition (and, in some cases, exclusively to vascular effects). This issue is independent of the imaging sequence of choice (T_2* or T_2 weighted) and makes the neurovascular interpretation much more complicated.

Models of neurovascular coupling have been proposed to aid in the interpretation of the BOLD signal changes. In particular, biophysical generative models (Havlicek et al., 2015) can be used to deconvolve the neuronal information from the measured fMRI (BOLD) activity. These models consider constraints derived from invasive recordings to infer the neuronal signaling (e.g. the EI balance) from fMRI measures. The development and use of these models have been based mostly on macroscopic scale fMRI measures with large voxels (> 2 mm isotropic) (see below for the current extensions to smaller scale measurements) (Fig. 2). In combination with careful experimental design and/or additional data from other imaging techniques (e.g. CBF and CBV), neuronal effects can be disentangled from spurious vascular contributions. The possibility of deconvolving the underlying neuronal effects from BOLD signal measures may allow using fMRI (instead or in addition to electrophysiology) to address questions that so far could only be tackled by invasive neurophysiology. Together with the large coverage achievable in fMRI, this will aid in validating computational models (based on neural mass models) aimed at understanding the large scale (e.g. across areas) computations that underlie brain function (Fig. 2). The ability to use fMRI instead of invasive electrophysiological

measures is fundamental to extend these studies from basic sensory processes to more complex (uniquely human) cognitive functions.

Biophysical modeling of the neurovascular coupling has already been adapted to consider the signal variations with field strength (Uludag et al., 2009). However, as the imaging resolution approaches the size of the cortical columns and layers, models of cortical neurovascular coupling need adapting (Goense et al., 2016). A simple model that considers the hemodynamic response of each layer to be uncoupled cannot explain the biases that are observed in the measured fMRI response (e.g. the increase in signal towards the surface of the cortex in GE based fMRI). For this reason, laminar and columnar fMRI is currently used for differential mapping and mainly in applications for which information is available from invasive recordings in animals. More accurate hemodynamic models require the consideration of draining effects in the cortical columns based on plausible models of the cortical vasculature together with other laminar differences relevant to the hemodynamic coupling (e.g. the different impact of CBV across layers or differences between positive and negative BOLD responses (Goense et al., 2012)). Some initial attempts in this direction have been performed with varying degree of sophistication (Gagnon et al., 2015; Heinzle et al., 2016; Markuerkiaga et al., 2016) and also considering the relationship between laminar fMRI and EEG (Scheeringa et al., 2016). But more work is needed in order to create accurate generative models at the mesoscopic scale (Fig. 2). Other issues such as the neurovascular coupling of different cell populations (e.g. excitatory vs. inhibitory neurons) may also become relevant for laminar investigations, as cells are differently distributed across cortical layers. When available, laminar models of neurovascular coupling will allow linking in vivo functional measures to neuronal computations at the mesoscopic scale and using fMRI for the development of accurate mesoscopic models (based on e.g. the canonical microcircuit) of human function (Fig. 2).

Analyzing functional responses

Since its introduction, fMRI provided neuroscientists with an unprecedented amount of data. Even at a resolution of 3 mm a functional scan of the whole brain contains tens of thousands of cortical voxels (i.e. gray matter voxels). For each voxel, responses can be collected with a temporal resolution that nowadays reaches the hundreds of milliseconds (Ugurbil et al., 2013). For this reason the development of fMRI acquisition techniques has been paralleled by a continuous and steady development of signal and image analysis techniques.

Fields of applications have also been increasing steadily through the years, supported by a multitude of possible experimental designs. The great majority of fMRI studies follow the standard approach of cognitive psychology based on cognitive subtraction, and uses related statistical methods for the analysis. In this scenario, brain responses are recorded in response to two or more experimental conditions (e.g. faces and houses, voices and music, visual gratings with different orientations, tones with different frequencies). Statistical differences between conditions are then assessed at level of single voxel responses (univariate, e.g. GLM) or voxel pattern responses (multivariate, e.g. MVPA, RSA, fMRI decoding) (see Fig. 3 and below). While useful for detecting differences between conditions, this type of discriminative analyses are not concerned with defining the computational operations that generate these differences.

The possibility of measuring the responses of populations of neurons with high tSNR and spatial specificity has provided the basis for developing methods that link fMRI responses and computational models of neural processing formally (Dumoulin and Wandell, 2008; Naselaris et al., 2010; Wandell, 1999). These methods offer the opportunity to model the computational properties of neuronal populations in sensory areas (i.e. population Receptive Fields (pRF), see below) and can be extended to test models of complex cognition (see e.g. (Keuken et al., 2015)) or hypotheses on the influence of cognitive processes (e.g. attention) on sensory processing (de Haas et al., 2014; Kay et al., 2015; Klein et al., 2014; Sprague and Serences, 2013).

In what follows we describe in more detail some of the more typical analysis choices and how moving the acquisition of the fMRI data to UHF influences them.

Analyzing differences between experimental conditions at single voxels

Most fMRI studies in cognitive neuroscience employ a technique that *maps* the differences between conditions at the level of individual voxels (i.e. univariate analysis) using statistical tests (within the framework of the General Linear Model [GLM]) (Friston et al., 1995) (Fig. 3). The statistical maps obtained from such analyses are thresholded by the significance (p value) of the statistical test after correction for the multiple (many thousands) of comparisons.

This analysis framework is limited by two factors. First, voxels must exhibit sufficiently strong response selectivity. In other words, the voxels have to sample a homogeneous neuronal population that respond preferably to one of the stimulus classes (e.g. human voices). This issue links the imaging resolution with the spatial scale of the information under investigation. Univariate analysis methods are suited when voxels (or regions of interest) sample neuronal activation at a scale close to the level under investigation. Second, statistical techniques are susceptible to the temporal variability in the voxels' functional responses (i.e. the temporal signal to noise ratio [tSNR]). The higher the *noise* contribution to the signal, the lower the probability of detecting statistically significant differences. Post-processing techniques can be used to improve statistical power under specific assumptions. In particular, at conventional field strengths (< =3 T), spatial smoothing is widely employed in fMRI data analysis under the assumption that the selectivity of the response is similar in neighboring voxels. Further, statistical inferences can be carried out across subjects (after spatial normalization to a template space), under the assumption that information is localized in corresponding (macro) anatomical locations across subjects.

Analyzing patterns of fMRI responses: MVPA and RSA

Multivariate analysis techniques have been introduced, motivated by the need of detecting effects of the stimuli that are not localized within a voxel (Haxby et al., 2001). In fMRI, this has been translated to the investigation of the (statistical) information present in a (distributed) collection of voxels (Fig. 3). The degree of spatial distribution of the effects over the brain ranges from a local neighborhood of voxels (searchlight analysis) (Kriegeskorte et al., 2006) to regions of interests (Haynes and Rees, 2005; Kamitani and Tong, 2005) and the whole brain (De Martino et al., 2008; Mourao-Miranda et al., 2005).

By considering the information within spatial patterns, multi voxel pattern analysis (MVPA) methods have an increased statistical power compared to standard univariate analysis (i.e. they perform weighted averaging of voxels). Furthermore, compared to conventional univariate statistics MVPA allows investigating how much information is shared across experimental conditions. For instance, using *cross-decoding* the shared information across sets of conditions can be assessed by training a classifier on one set of conditions and then testing its performance on another set of conditions. In (Formisano et al., 2008), for example, a classifier was trained with vowels spoken by one speaker and tested on the same vowels spoken by a different speaker, to assess to what extent pattern information is robust to acoustic variation.

In some cases MVPA has been used to infer information at a finer spatial scale than the imaging resolution (e.g. investigating columnar level information such as the orientation of visual gratings from low resolution [3 mm isotropic] voxels). It was proposed that this was

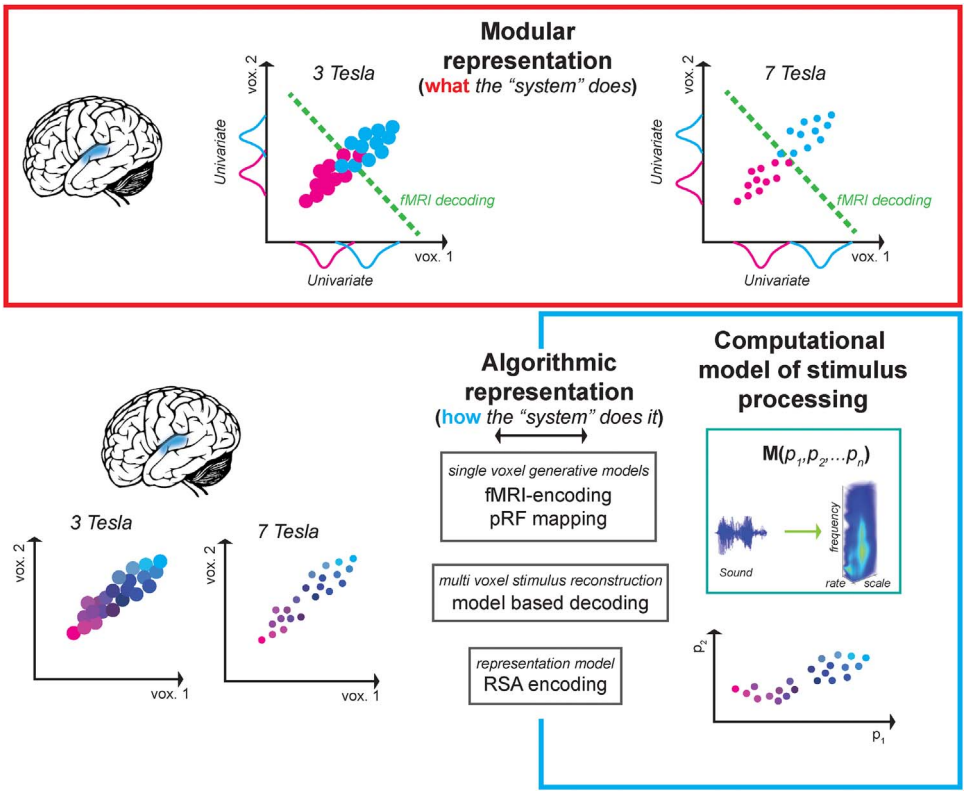

Fig. 3. fMRI analysis methods and the way that high magnetic field measures affect them. Univariate statistical analysis (i.e. GLM) and multivoxel pattern analysis (MVPA) investigate differences between conditions (blue and pink dots in the top panel). High field acquisitions improve single trial estimates due to the higher temporal signal to noise ratio and improve separation between classes due to the increase specificity. Computational neuroimaging approaches allow linking in vivo measures of brain functions with computational models (bottom right panel). The higher temporal signal to noise available at high fields improves the estimation of responses to single stimuli and improves the estimation of the representational geometry. This benefits both representational similarity type of analysis as well as computational neuroimaging approaches that link the representational geometry (at single or multiple voxels) with the model representation.

possible because of *hyperacuity*: voxels exhibit small but stable biases in their response to two (or more) conditions (Kamitani and Tong, 2005). Hyperacuity and its (neuronal) origin have been the matter of much debate in the fMRI literature (Chaimow et al., 2011; Freeman et al., 2011; Kriegeskorte et al., 2010; Op de Beeck, 2010a, 2010b). In particular, interpreting results from low resolution decoding as being dependent on high-resolution information (e.g. columnar or laminar) has one fundamental limitation. The discriminative power of the analysis is affected by information from any (neuronal or vascular) source that (1) is correlated with the source of interest, and that (2) may be present at a lower spatial scale. For example, the MVPA analysis of visual orientation may have been confounded with radial biases in the discrimination of grating orientations (Sasaki et al., 2006) (but see e.g. (Alink et al., 2013)).

By abstracting from the response to a single stimulus or to a stimulus category, representational similarity analysis (RSA) characterizes the information present in a brain area (or searchlight location) through the stimulus representational geometry (i.e. the representation (dis)similarity matrix [RDM] that is the distance between the stimuli in the space of the fMRI patterns) (Kriegeskorte et al., 2008). RSA can be used to relate different imaging modalities (e.g. fMRI and MEG), or to relate the information within homologous areas across species. The stimulus representational geometry can be used to compare brain activity (i.e. fMRI based) to stimulus based representation. If the stimulus representation being considered is categorical (i.e. consisting of discrete classes e.g. objects, faces) (Kriegeskorte et al., 2008) then the RDM analysis reduces to a multi-voxel decoder based on correlation that weights all voxels equally. However, the approach can be extended to consider a continuous representation of the stimuli based on a computational model (see below)(Anderson et al., 2016).

Linking fMRI data and computational models: pRF mapping fMRI encoding and model based decoding

Brain inspired computational models are formal (algorithmic) representations of the processes associated with a specific brain function (e.g. visual object recognition, sound recognition). For sensory processing they can be seen as the representation of the stimuli **S** as a function of the model features p_i (see Fig. 3). It can be argued that an *accurate* model of the computations enabling a given process should allow explaining observed responses in the brain locations where that process is instantiated. The aim of such a modeling approach is to predict observed response levels and patterns for a large number of individual stimuli, and not simply to detect the (average) response differences between stimulus classes, as typically done with the GLM or MVPA (Naselaris and Kay, 2015).

In fMRI, several strategies have been used to link formal computational models to brain activation. Population receptive field (pRF) mapping (Dumoulin and Wandell, 2008) is a fully generative model that calculates neuronal population responses from a stimulus representation, using a fully parameterized population receptive field (e.g. a Gaussian function in the visual field). The prediction of fMRI responses, at a single voxel, is obtained by convolving the modeled neuronal response with the hemodynamic response (see e.g. (Kay et al., 2013b) and Appendix A for more details). Crucially this technique allows for the inclusion of parameterized non linear transformations (Kay et al., 2013a, 2013b). This method has been used to estimate pRFs in visual (see e.g. (Dumoulin and Wandell, 2008; Kay et al., 2013b)), auditory (Thomas et al., 2015), and parietal cortex (Harvey et al., 2013) and requires non-linear optimization techniques with high computational load.

fMRI encoding considers a linearized representation of the fMRI

response of a voxel as function of the stimulus representation model (see Appendix A for details on how it relates to pRF modeling). This approach has been used to predict the fMRI response of voxels in visual (Kay et al., 2008) and auditory cortex (Moerel et al., 2012; Santoro et al., 2012). Note that in fMRI encoding the population receptive field shape is not assumed and thus it is possible to detect complex pRF shapes (see e.g. (Moerel et al., 2013)). Single voxel encoding models (or pRF models) allow predicting the response to new stimuli. Single voxels prediction can be combined for decoding multivoxel response patterns (Naselaris et al., 2010). Importantly, encoding models allow resolving some of the ambiguities introduced when using MVPA such as the influence of different factors (cognitive or stimulus related) to the classification performance (see (Naselaris and Kay, 2015) for more details).

Functional MRI encoding and pRF mapping allow characterizing single voxels as a (linear) function of model features. Thus – similarly to GLM analysis - they become more meaningful at high spatial resolutions when the neuronal population sampled is more homogenous in terms of their receptive field. Issues introduced by the high dimensionality of the model space or the correlation between model features can be resolved using regularized fitting techniques. An assumption of these methods is that the stimulus features that maximally contribute to a voxel response are also those encoded with greatest fidelity. However, as discussed in the case of multivariate decoding, detection of information about a stimulus (or a stimulus feature) can be optimized by considering spatial response patterns rather than single voxels. This is done within *model based decoding* where features of the stimulus model based representation are the dependent variables and the fMRI response patterns are the independent variable of a linear regression (Miyawaki et al., 2008). With this approach, features of the stimulus representation model are directly decoded by fMRI response patterns allowing direct stimulus reconstruction (e.g. the reconstruction of the picture seen (or sound heard) by the subject on the basis of the pattern of responses). As a drawback, model features are fitted and predicted independently from one another and thus the correlation between them is not considered explicitly. It has to be noted that using this approach, model comparison can be conducted after recombining all the predicted stimulus representation features and performing a stimulus identification analysis in the space of the model features.

Moving to ultra high fields and high resolution - Consequences for data analysis

Moving to higher magnetic fields provides an increase in sensitivity (i.e. SNR). When physiological noise does not dominate (e.g. for high resolution imaging), the increase in SNR translates directly into an increase in temporal signal to noise (tSNR) (Triantafyllou et al., 2005). While careful considerations have to be made depending on the source of the functional contrast (T_2* or T_2 weighted) and the image resolution, UHF imaging also grants an increase in the specificity of the signal (see above and Table 1). At 7 T a voxel volume of 4 mm^3 (1.6 mm isotropic) provides similar sensitivity as a 8 mm^3 (2 mm isotropic) voxel volume at lower fields (but increased specificity and contrast to noise; see e.g. protocols at http://www.humanconnectome.org/). Increasing resolution further comes at the expense of sensitivity (tSNR) but GE-EPI based acquisitions at about 1.3 mm^3 (1.1 mm isotropic) are still practical at 7 T even in subcortical areas (Moerel et al., 2015b). Submillimeter acquisitions at 7 T are low in SNR compared to conventional 3 T acquisitions. For this reason, submillimeter fMRI requires careful considerations regarding the FOV and acceleration factor in order not to compromise the effective resolution or the tSNR excessively.

Taken together, these changes have direct consequences for the analysis of fMRI data. When high-resolution data are acquired at 7 T, the higher number of voxels (e.g. reducing voxels resolution from 2 mm isotropic to 1.6 mm isotropic results in two times more voxels when considering equivalent volume coverage) increases the computational cost and, for univariate analyses, the number of statistical tests that are performed.

Table 1
Comparison between 7 T and 3 T sensitivity and specificity for both T2* and T2 weighted type of acquisitions. The plus sign indicates a benefit for 7 T.

	T_2* weighted		**T_2 weighted**	
7 T vs. 3 T resolution	*Same*	*7 T higher than 3 T*	*Same*	*7 T higher than 3 T*
SNR	++	~	++	~
tSNR	++ / +	~	++/+	~
Specificity	~	+	++	+++

When considering the same imaging resolution moving to 7 T results in an increase in SNR (++). How this translates to increases in tSNR depends on the regime at which images are acquired (see e.g. Triantafyllou et al., 2005 for a quantitative analysis). In the thermal noise dominated regime (e.g. high resolution imaging) SNR increases translate to equivalent tSNR increases (++). In the physiological noise dominated regime (e.g. low resolution) the tSNR increase is more moderate (+). Acquiring higher resolution images at 7 T trades SNR for increases in specificity due to partial volume effects (+ for T_2* weighted acquisitions). T_2 weighted acquisitions are generally more specific at 7 T compared to lower fields (++) and benefit from the possibility of acquiring higher resolution images by reducing partial volume (+++).

The higher sensitivity can translate to more statistical power for univariate statistical modeling (Fig. 3). For applications that require high tSNR at conventional fields (i.e. when physiological noise does not dominate), the higher SNR available at UHF results in increased tSNR. Other sources of variability (e.g. the “neuronal” variability in response among different stimuli belonging to the same class) are not affected by the field change. As a result of the increased tSNR, for single voxels, the responses are more easily detectable at high fields.

Specificity of fMRI responses to neuronal effects is affected by imaging resolution, by the BOLD point spread function (Shmuel et al., 2007) and by the spatial distribution of the effects under investigation. If high-resolution information is being studied (e.g. orientation or ocular dominance columns in V1), increasing resolution increases the selectivity of the voxels’ responses (i.e. the difference between stimulus classes in Fig. 3). At lower field strengths (3 T) and with large voxels, multivariate methods have aided the detection of weak and spatially non-uniform univariate effects. In such cases, the increase in selectivity obtained with UHF likely allows using univariate statistical mapping, with a consequent simplification in the interpretation of resulting maps. Multivariate methods, however, are still useful for examining effects that are not encoded in the response levels but, e.g. in the correlations across voxels (i.e. ‘truly’ multivariate effects).

With UHF fMRI, similar improvements can be expected for MVPA (Fig. 3). When physiological noise does not dominate the signal fluctuations, the higher tSNR available at high fields guarantees more accurate estimates of brain responses, even for single trials. Further, depending on the interaction between imaging resolution and the scale of the pattern under investigation, the higher specificity may results in larger differences among classes of stimuli (Andersson et al., 2011; Beckett et al., 2012; Gardumi et al., 2016; Stelzer et al., 2014).

For RSA, the higher tSNR permits a better definition of the stimuli representational geometry based on brain responses (e.g. better estimation of the brain-based dissimilarity matrices) and results in a reduced effect of the noise on model evaluation (i.e. increased noise ceiling) (Nili et al., 2014). This benefits also pRF modeling fMRI encoding and model based decoding analyses. As a result, high field data could allow more accurate model comparisons in situations in which two or more competing models are being investigated (Santoro et al., 2014). Finally, the higher specificity and higher spatial resolution allow measuring voxels with a more homogenous distribution of voxels in terms of their receptive fields. This is advantageous for both pRF

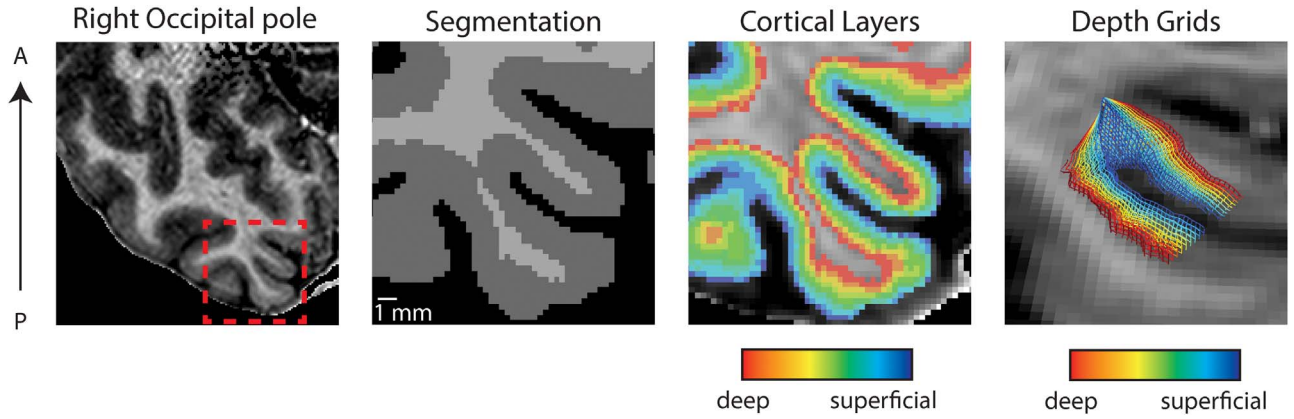

Fig. 4. Definition of cortical layers based on in vivo anatomical data collected at 9.4 T (0.35 mm isotropic). Starting from the original data (left), a segmentation procedure is used to define both white and gray matter (second from left). Within the gray matter ribbon the equi-volume approach was used to define cortical layers from deep to superficial (red to blue, third from left). The volumetric definition can be used to obtain cortical grids that vary from deep to superficial cortex (right).

modeling and fMRI encoding that can model the fMRI responses for neurophysiologically plausible computational units (e.g. columns and layers in the cortex).

Developing tools for high resolution (submillimeter) fMRI analysis

The investigation of cortical depth dependent neuronal responses with fMRI (i.e. laminar and columnar fMRI) requires acquiring and analyzing functional and anatomical data at submillimeter resolution. In such contexts, the use of standard pre-processing steps (e.g. spatial smoothing, normalization to a template) has to be carefully considered (Turner, 2016).

To make the best use of the high-resolution data acquired, in recent years the conventional analysis pipelines have been modified and new tools developed. The analysis of cortical depth dependent fMRI data requires an accurate definition of the cortical ribbon (i.e. both the white/gray matter boundary and the gray matter/cerebrospinal fluid boundary). In conventional structural analyses, e.g. in the analysis of gray matter cortical thickness, this information can be extracted from high-resolution anatomical data acquired with sequences that are free of most of the geometric distortions arising from EPI-based acquisitions (e.g. magnetization prepared rapid acquisition gradient echo [MPRAGE]). Conversely, in high-resolution fMRI applications there is the need to co-register submillimeter *functional* and *structural* data. This has pushed the development of new methods that allow accounting for the different geometric distortion between the two image types.

Currently, three different approaches have been proposed to deal with this issue. The first corrects for geometric distortions in the functional images and aligns them to the (higher) resolution anatomical images that are (relatively) distortion free (see e.g. (Emmerling et al., 2016)). The second approach uses anatomical images that are "distortion matched" to the functional images (e.g. T1 weighted images acquired with an EPI readout) (see e.g. (Renvall et al., 2016)) The third segments the functional data directly (see e.g. (Fracasso et al., 2016)). In all cases, considering a limited region of interest, to drive the alignment and/or to segment the data can be beneficial (Kemper et al., 2015).

Several methods have also been developed for the sampling of cortical depth dependent responses from the high-resolution fMRI data. The explicit representation of meshes (Polimeni et al., 2010) or regular grids (Zimmermann et al., 2011) at different cortical depths can be used to re-sample the functional responses to a new three-dimensional space that varies both tangentially (within a lamina or at a cortical depth) and perpendicularly (across laminae, in radial direction) to the cortical ribbon. In the standard mesh approach vertices of a mesh are created from a (voxelated) segmentation of the gray/white matter boundary. The number of neighbors of a vertex varies depending on the originally reconstructed voxel boundaries. After smoothing the mesh, this variation leads to inhomogeneous density sapling, i.e. different distances and angles between edges formed by the triangles, which connect a vertex with its neighbors. Regular grids, on the other hand, are created explicitly following an iso-surface at middle cortical depth. Each grid point has 4 constantly spaced neighbors forming approximately 90 degree angles between edges. Note that distances stretch or shrink as in the mesh approach when grids are evolved across cortical depth depending on local cortical curvature. The explicitly created regular grids simplify post-processing of sampled functional data such as shortest distance, gradient and curvature calculation but are appropriate only for small regions of interest (for more detail see (Kemper et al., 2017)).

By analyzing the signal variability within and across cortical depths, high-resolution fMRI data can be used to investigate the existence of functionally homogeneous cortical columns (De Martino et al., 2015; Nasr et al., 2016; Zimmermann et al., 2011) and reveal cortical depth dependent processing (De Martino et al., 2015; Muckli et al., 2015). Fig. 4 shows the definition of depth dependent grids in a region of interest of the right occipital pole. The partition of the cortical ribbon into different cortical depths or laminae can also be obtained in volumetric space. This has been used to analyze the changes across depths within defined regions of interest (Kok et al., 2016; Koopmans et al., 2010, 2011; Siero et al., 2011).

For either surface- (grid-) or volume-based approaches, different methods can be used to assign voxels to specific 'laminae'. Responses can be re-sampled from equi-distant partitions (relative to the cortical depth) of the cortical ribbon (Kemper et al., 2015, 2016; Koopmans et al., 2010, 2011; Polimeni et al., 2010; Siero et al., 2011). More recently, volume-preserving techniques have been developed (Waehnert et al., 2014) to respect the changing position of cortical laminae depending on changes in curvature. The Grids presented in Fig. 4 were extracted using an equi-volume definition of the cortical laminae. While the advantage of the second technique has been clearly shown at very high spatial resolution (< 200 μm), the difference between the two techniques becomes smaller at the resolution of conventional submillimeter fMRI acquisitions (0.8 mm isotropic) (Guidi et al., 2016).

fMRI at ultra high fields, example applications

In what follows we will present an overview of 7 T fMRI applications of both cortical and subcortical processing. Examples of cortical applications are further subdivided according to imaging resolution and cognitive functions including basic perception. A more specific focus on perception can be gathered from the review of Dumoulin et al. (submitted to this special issue).

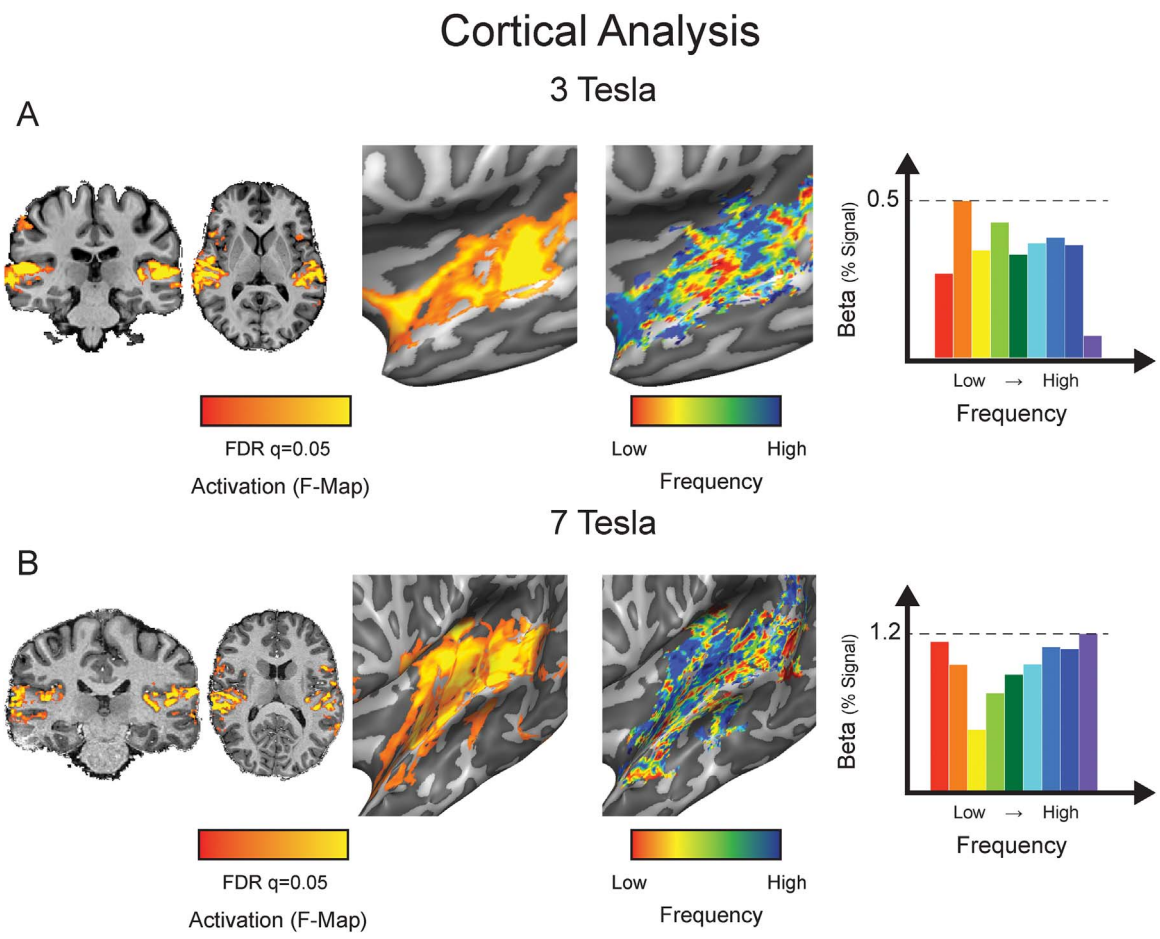

Fig. 5. Example of fMRI data acquired at different field strengths. The presentation of amplitude modulated tones at different frequencies activates the human auditory cortex (left panel). Tonotopic maps (central panel) result from color-coding (red-green-blue for low-mid-high frequencies) vertices based on the frequency eliciting the strongest response. Response estimates in the most medial portion of Heschl's gyrus (right panel, percent signal change) are obtained with a GLM analysis including a predictor for each frequency. Results obtained A) at 3 T with a 2 mm isotropic acquisition (data analyzed at 2 mm isotropic). and B) at 7 T (1.5 mm isotropic acquisition and data acquired at 2 mm isotropic to match the resolution of the 3 T data), Note that 7 T acquisition results in more detailed maps and higher percent signal change as a result of the slightly increased specificity caused by the higher resolution of the acquisition and the improved statistical power resulting from the higher sensitivity.

Investigations of cortical processing with voxel volumes above 1 mm^3

Several studies have used fMRI data at 7 T to investigate cortical function seeking to increase statistical power or decoding accuracy compared to similar lower field studies while improving spatial resolution (see Fig. 5 panel A and B for a comparison between a comparable study run at 3 T and 7 T).

Investigating the function to structure relationship and resting state connectivity

The increased anatomical contrast available at high fields has allowed researchers to map myeloarchitectinic information in vivo and with great detail (Geyer et al., 2011; Turner, 2016). These techniques (in combination with functional measures of resting state connectivity) have been used at lower field strength to produce a detailed in vivo parcellation of the human cortex (Glasser et al., 2016). At UHF the relationship of anatomical areal markers (e.g. high myelin-related contrast, layer dependent myelin-related profiles) to functional characteristics has been investigated in early visual (Sanchez-Panchuelo et al., 2012b), auditory (De Martino et al., 2014) and somatosensory cortices (Sanchez-Panchuelo et al., 2014) and promises to be relevant to the investigation of other cortical areas. The high temporal signal-to-noise and/or resolution have also benefitted applications to the analysis of functional connectivity during rest (De Martino et al., 2011; Hale et al., 2010).

Cortical topographic maps of perceptual processes

Pioneering neuroscience applications at 7 T investigated the topographic responses (tonotopic maps) to sound frequencies in the human auditory cortex (Formisano et al., 2003). Mapping the topographic responses of other sensory cortices rapidly followed suit. Retinotopic maps in visual areas have been obtained at 7 T and compared across field strengths and for different acquisition types (T2* and T2 weighted) (Hoffmann et al., 2009; Olman et al., 2010). In the somatosensory cortex 7 T has been used for mapping single digit information (Martuzzi et al., 2014; Sanchez-Panchuelo et al., 2010; Siero et al., 2014; Stringer et al., 2010; van der Zwaag et al., 2015), topographic representations of different phalanges (Sanchez-Panchuelo et al., 2012a), and the mechanoreceptive afferent units in the median nerve (Sanchez Panchuelo et al., 2016). Making use of the high temporal signal to noise of UHF fMRI, other aspects of sensory processing have investigated, for example, the cortical responses to sound position (van der Zwaag et al., 2010), the processing of tactile motion (Wacker et al., 2011), the involvement of the somatosensory cortex in observed touch (Kuehn et al., 2013), the representation of simple and complex movements in both sensory and motor cortices (Ejaz et al., 2015), the presence of information over action preparation in visual cortex (Gutteling et al., 2015), and the relevance of a predictive code for motion in early visual cortex (Schellekens et al., 2016).

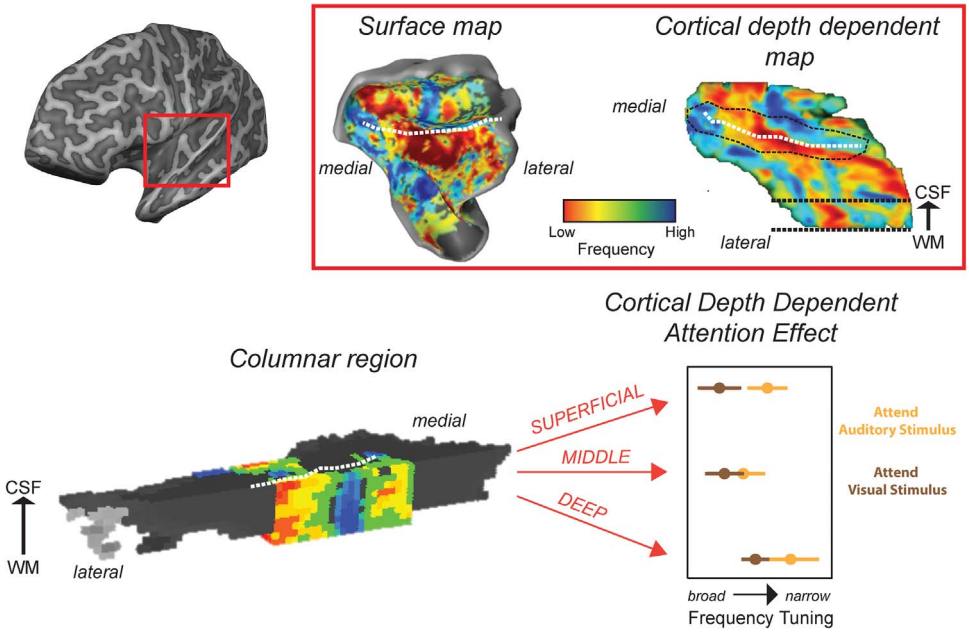

Fig. 6. Example of mesoscopic scale fMRI. Pushing the resolution of the acquisition below the cubic millimeter (7 T data acquired at 0.8 mm isotropic with 3D-GRASE) allows detecting the columnar organization of the human primary auditory cortex. Tonotopic maps can be reported on one surface (surface map) by e.g. averaging across cortical depths. Making use of the full depth information allows rendering the tonotopic map (cortical depth dependent map). Analyzing the gradient of frequency preference radially and tangentially to the cortical surface allows highlighting columnar (i.e. less variable across depths than tangentially) regions. Cortical depth dependent fMRI data allow investigating the influence of higher level cognitive processes (e.g. attention) on sensory stimulation. In tonotopic columns, attention to the relevant stimulus (auditory) sharpens the frequency selectivity (narrower tuning) in superficial layers but not in middle or deep ones.

Computational modeling of perceptual processes

In combination with computational modeling approaches 7 T measurements have permitted investigations of the population receptive field responses in auditory cortex, highlighting complex frequency dependent responses (Moerel et al., 2012) and their relevance for the processing of pitch chroma (Moerel et al., 2015a). The high sensitivity has allowed for more accurate model comparison in determining the relevance of spectro-temporal modulations to the processing of natural sounds (Santoro et al., 2014). For a review of applications to the modeling of the population receptive fields in visual cortex using UHF we refer to (Dumoulin et al., 2017). Computational approaches have also been used to investigate the topographic representation of numerosity (Harvey et al., 2013) and its relationship to object size (Harvey et al., 2015). Finally the high tSNR granted by UHF has been used to investigate the functional connectivity between visual areas and its relationship to population receptive fields (Haak et al., 2013).

Imagery, decision making and mental orientation

High tSNR available at UHF has also been at the basis of the investigation of the multivariate information present in sensory areas for imagined stimuli (e.g. imaginary motion) (Emmerling et al., 2016) or the unconscious generation of free decisions in frontal cortex (Bode et al., 2011).

Taking advantage of the increased spatial resolution compared to lower fields, UHF fMRI has revealed a topographic representation in the precuneus and inferior parietal lobe for mental orientation towards space, time and person (Peer et al., 2015).

Language processing

In a recent study the increases sensitivity of 7 T fMRI has been sued to study the effect of oscillatory phase on the representation of syllables (Ten Oever et al., 2016). High sensitivity, obtained at 7 T, and high temporal resolution have also been used in order to decode words from multivariate patterns in temporal cortex (Vu et al., 2016b).

Attention modulation of sensory information

Investigating the representation of sensory input is a standard application of fMRI. The way that these representations are modulated by task or attention has also been a matter of extensive research. In this respect the complexity of the fMRI signal and its sensitivity to neuromodulatory signals (Logothetis, 2008) may represent a benefit. UHF fMRI permits investigating how neuromodulatory inputs affect sensory processing at the level of large-scale topographic responses (auditory and visual) (Da Costa et al., 2013; Schallmo et al., 2016) and the biased sampling of fine-grained information (i.e. visual orientation) (Warren et al., 2014). In combination with a computational modeling approach (i.e. pRF mapping), UHF fMRI has been used to investigate the changes in the population receptive fields (e.g. location) induced by attention (Klein et al., 2014).

Investigating the source of multivariate information in fMRI

The possibility of measuring responses at higher spatial resolution and with high sensitivity has also inspired investigations of the "hyperacuity" of MVPA (see section "Analyzing patterns of fMRI responses: MVPA and RSA") by analyzing the multivariate information content at different spatial scales (Beckett et al., 2012; Gardumi et al., 2016; Swisher et al., 2010).

Investigations of cortical processing with voxels volumes below 1 mm^3

Pushing the limits of spatial resolution below a cubic millimeter allows the investigation of the computational architecture of the cortex at the level of layers and columns (Fig. 6). Interestingly, this level of imaging greatly facilitates investigating the influence of higher level of cognitive processes (e.g. attention) on early sensory processing (Fig. 6).

High resolution (depth dependent) maps of sensory processing

Using isotropic resolution and multiple slices, submillimeter fMRI has been used to map the functional organization for binocular disparity averaged across middle cortical depths (i.e. no cortical depth

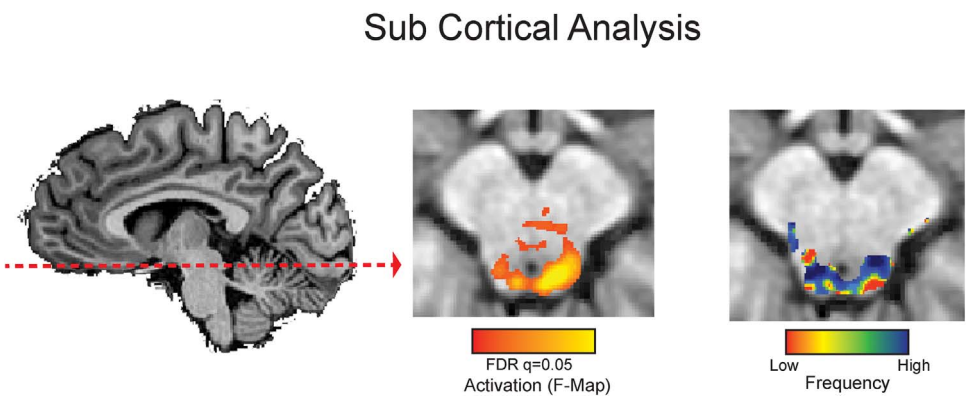

Fig. 7. The higher sensitivity available at higher magnetic fields allows mapping the functional organization of subcortical structures. The human inferior colliculus (IC) responds to the presentation of amplitude modulated tones (Activation map in the middle) and color-coding (red-green-blue for low-mid-high frequencies) voxels based on the frequency eliciting the strongest response allows detecting the spatial arrangement of preference for sound frequencies (tonotopy) in the IC (right).

dependent representation) (Goncalves et al., 2015) and to investigate cortical depth dependent signal changes (e.g. laminar fMRI) in visual and auditory cortex (Ahveninen et al., 2016; Polimeni et al., 2010).

The relevance of laminar processing has also been investigated by looking at the information content for intact and scrambled objects (Olman et al., 2012) and stimuli preferentially activating magno- and parvo- cellular layers of primary visual cortex (Olman et al., 2012).

Cortical columns

Early pioneering work has shown how high resolution fMRI at 7 T can allow mapping ocular dominance columns (Yacoub et al., 2007) and orientation domains (Yacoub et al., 2008) in primary visual cortex. Albeit limited to a single slice of cortex, these early applications have also been used to showcase the specificity differences between T_2* and T_2 weighted acquisitions (Yacoub et al., 2007). Even when using multiple slices, the issue of the specificity of the signal changes has remained a central topic in the field and several studies have investigated T_2 weighted and T_2* weighted BOLD (De Martino et al., 2013b; Kemper et al., 2015, 2016; Koopmans et al., 2011) and analyzed the specificity of signal changes related to blood volume (Huber et al., 2015). Leveraging the high resolution, cortical columns have been mapped in humans for the first time outside striate visual cortex, mapping the axis of motion preference in the human middle temporal area (Zimmermann et al., 2011), the tonotopic preference in auditory cortex (De Martino et al., 2015), and color and disparity columns (Nasr et al., 2016). Fig. 6 shows an example of columns in human primary auditory cortex (PAC) exhibiting homogeneous frequency preference. The data collected at 0.8 mm isotropic resolution (3D-GRASE, see (De Martino et al., 2015) for details) have been analyzed in the volume space and maps are sampled on equidistant cortical grids rendered as a three-dimensional cube to aid visualization (and analysis) of columnar structures.

Layer dependent modulatory information on sensory processing

Submillimeter fMRI at UHF has allowed investigating the modulation of the cortical depth dependent fMRI signals in primary auditory and visual cortices in relation with attention (De Martino et al., 2015; Kok et al., 2016). Fig. 6 highlights the depth dependent modulation of frequency tuning in human PAC with respect to the task demands. When attending the relevant auditory input superficial layers of PAC sharpen their frequency tuning allowing a better representation of the stimuli.

Using similar techniques (i.e. cortical depth dependent sampling of functional information) investigators have also reported the relevance of superficial layers in processing contextual feedback in early visual cortex (Muckli et al., 2015).

Investigations of subcortical and cerebellar processing

The higher sensitivity available at 7 T has greatly benefitted investigations of subcortical and cerebellar processing. Applications have focused on both basic sensory and motor processing as well as higher order cognition (e.g. emotion, decision making and memory) and respiratory control (Faull et al., 2015). Additionally, resting state connectivity of thalamic and subcortical regions has also been investigated (Bianciardi et al., 2016; Maass et al., 2015; Torrisi et al., 2015), along with its correspondence to anatomical connectivity (Lenglet et al., 2012).

Subcortical and cerebellar topographic maps of perceptual processes

The increase in spatial resolution, obtainable at ultra high fields, has allowed mapping the functional topography of subcortical and cerebellar structures. Fig. 7 presents, as an example, the topographic representation of sound frequency in the human inferior colliculus mapped with GE-EP at 1.5 mm isotropic (for details see (De Martino et al., 2013a)). Functional studies at 7 T has also revealed tonotopic maps medial geniculate body (Moerel et al., 2015b), and the magno- and parvocellular subdivisions of the LGN (Denison et al., 2014) and the involvement of the superior colliculus in saccadic execution (Krebs et al., 2010). In the cerebellum, the somatotopic representation in the dentate nucleus has been reported (Kuper et al., 2012) down to single digits representations (van der Zwaag et al., 2013). Functional MRI at 7 T has also been used to map the motor subsystems in the cerebellum (Batson et al., 2015) and the activation in cerebellum to sequential finger movements (Stefanescu et al., 2013). Finally, using fMRI encoding computational models for sound frequency and location in subcortical auditory structures (Moerel et al., 2015b).

Higher order cognitive processes: emotions, decision-making, memory, conflict resolution, arousal and expectations

The relevance of subcortical processing in higher order cognition has also been investigated using UHF fMRI. Subcortical structures have been implicated in the processing of arousing visual stimuli (Walter et al., 2008). The involvement of the subthalamic nucleus in decision making has been reported (Keuken et al., 2015), as well as activation of thalamic nuclei (Metzger et al., 2010) and the amygdala (Sladky et al., 2013; van der Zwaag et al., 2012) in relation to the processing of emotions. Several models have hypothesized that the increase of alternative choices is modulated by increased activity in the subthalamic nucleus (STN). In a recent study, one such model based on the multiple sequential probability ratio test has been has been used to accurately predict the fMRI activity of the STN acquired at UHF (Keuken et al., 2015), indicating a precise computational role for the STN in the process of decision making. In the striatum, a gradient has been reported in the anterior to posterior direction with more anterior

regions involved in higher level cognitive processes (Mestres-Misse et al., 2012). A network of subcortical structures has also been identified in relation to the processing of unexpected events (Mestres-Misse et al., 2016). Finally, several studies have focused on the functional subdivisions of the human hippocampus and their relevance in associative learning (Suthana et al., 2015) and episodic encoding (Berron et al., 2016; Maass et al., 2014). Note that, because of its anatomical location, the hippocampus shares the same imaging challenges as subcortical structures (e.g. distance from the receiving elements in the radio frequency coil and small size).

Discussion and future outlook

Functional magnetic resonance imaging has revolutionized the study of human brain function. After more than twenty years of investigations, the shear number of applications of fMRI to the study of perception and cognition is a testament to the utility of the method (Fig. 1). The main criticism to fMRI, its indirect link to neuronal activity, is slowly being resolved through simultaneous recordings of fMRI and electrophysiology (Logothetis et al., 2001) and invasive animal (optical) recordings (O'Herron et al., 2016).

High magnetic fields offer increased sensitivity. This alone provides a tremendous advantage for applications that are starved by poor signal-to-noise at conventional field strengths. The study of subcortical function is a clear example of an application that was in need of SNR, and has already benefitted from high field fMRI. Trading sensitivity for resolution in turns allow for increased spatial specificity. This further benefits the interpretability of the results, as computational processes that were mixed within large voxels now become distinguishable. This is fundamental to investigate higher cognitive functions as the higher resolution allows investigating functional subdivisions for higher cognitive processes (e.g. univariate mapping) in approaches similar to the ones that have been used for sensory mapping. Striking the right balance between resolution and tSNR allows using simpler analysis strategies such as univariate statistical tests in situations where MVPA was required at lower field strengths. In combination with modeling approaches UHF can allow testing computational models of both sensory and higher order cognitive processing and the increased specificity of UHF increases the confidence that the results depend on the underlying neuronal processes rather that spurious vascular artifacts.

Pushing fMRI spatial resolution to below a cubic millimeter opens up an unprecedented spatial scale for non-invasive in vivo investigations of human brain function (Fig. 2). While the specificity of the signal depends on the acquisition details (e.g. T_2^* or T_2 weighted acquisitions), submillimeter fMRI acquisitions enable examining the architecture of the human brain at the level of cortical columns and layers. It has been shown in electrophysiological studies that columns represent fundamental computational units in many areas of the cortex (Hubel and Wiesel, 1968; Mountcastle, 1997). Hence, for the first time we have the ability to measure activity at the resolution of columns in humans using non-invasively in humans, which offers unprecedented opportunities to investigate fundamental aspects of neuronal computations. Initial studies (De Martino et al., 2015; Nasr et al., 2016; Zimmermann et al., 2011) have mainly focused on sensory areas with known columnar-level architecture from animal physiology but future studies may unravel columnar-level organizations in areas that are more specific to the human brain and for higher cognitive processes. Furthermore, computations in the human cortex also vary across cortical layers. Segregating functional responses across cortical layers allows investigating computations carried out within columns (e.g. the emergence of more complex processing in sensory areas) or understanding the interplay between feed-forward and feedback information (e.g. in the selection of behaviorally relevant stimuli) (De Martino et al., 2015; Kok et al., 2016; Muckli et al., 2015). The relevance of the layered architecture of the cortex outside of primary sensory areas and for higher cognitive processes can now be tested. In the field of decision making, for example, cells capturing decision input and output have been suggested to reside in different layers of the orbitofrontal cortex (Xie and Padoa-Schioppa, 2016).

Data acquired at the resolution of columns and layers not only more likely reflect existing computational models as fundamental computational units can now be mapped directly onto fMRI data, but can also help in informing and refining brain inspired computational models, e.g. by indicating which stimulus features and processing mechanisms the human brain uses to perform a given task. Until now invasive recordings have represented the gold standard for studying the brain at the scale of columns and layers, but these methods do not come without shortcomings. For example, when measuring spikes and spike rates, it is not easy to ascertain where the neuron is precisely located (unless small electrolytic lesions are left – identified in a post-mortem analysis). Further, local field potentials were found to be not so “local” after all (Kajikawa and Schroeder, 2011), while current source densities may be more spatially accurate but rely on a number of assumptions (Kajikawa and Schroeder, 2011, 2015). Thus, in some cases the precise localization of cortical layers is difficult, and data are often assigned to three classes (granular, supra-granular and infra granular) (Roberts et al., 2013). A similar picture can be obtained ultra high field when sampling functional responses at high-resolution. The obvious advantage of UHF is the ability to measure these responses non-invasively and in humans.

In conclusion, while UHF brings undisputable advantages to investigations at a spatial resolution above 1 mm, the most exciting and unique application lies in the laminar and columnar investigation of the human cortex. The improvements in the definition of the functional architecture of the cortex obtained using UHF are paralleled by the increased ability of obtaining meaningful cortical subdivisions from anatomical measures (see e.g. (Geyer et al., 2011)) allowing to complement the functional characterization of cortical areas with an anatomical fingerprint and examining the functional to anatomical relation in vivo and non invasively.

Translating the experiences made in early sensory areas with high-resolution functional imaging to both higher cognitive and uniquely human functions requires gaining confidence in the interpretability of the results obtained with fMRI. For these applications the possibility of confirming experimental data collected with fMRI in humans with invasive electrophysiological recordings will be, if at all, scarce. Ultimately, a layer dependent generative model that accounts for the empirical evidence that has shown differences in hemodynamic and neuronal processes across layers. Such a model would permit interpreting fMRI data in absence of prior electrophysiological evidence. Gathering the type of data necessary for the development of a mesoscopic neurovascular coupling model is not straightforward. While animal models are used for invasive electrophysiological recordings, the applicability of a neurovascular coupling model validated in animals (i.e. using both animal electrophysiology and animal fMRI) to human non-invasive measures will require careful considerations. Species differences in the neuronal distribution across laminae, the vascularization of the cortex and the effect of neuromodulatory signals are only some of the variables that would need to be taken into account in this passage. The same considerations apply when human fMRI data would be used together with animal electrophysiology in the modeling efforts. Collecting invasive electrophysiological measures in humans (e.g. electrocorticography [ECOG] or even laminar recordings) represents a rare but invaluable source of information in these efforts. Finally, the ability of laminar neurovascular coupling models to generalize across functions and areas would require testing in order to increase the possibility for cognitive neuroscientists to explore functions that are uniquely human and cannot be (easily) replicated in animals.

To extend the current effort in imaging the mesoscopic scale of information processing in humans outside primary sensory regions,

larger coverage acquisitions without compromised resolution and/or specificity will be key. This will allow extending principles such as columnarity and layer-specific processing to higher level cortical areas. Finally, in analyses of large scale connectivity, submillimeter fMRI will add a new dimension (cortical depth), which may help disambiguating the direction of information flow between connected locations.

Acknowledgements

This work was supported by the Netherlands Organization for Scientific Research (NWO; VIDI grant 864-13-012 to F.D.M., VENI grant 451-15-012 to M.M. and VICI grant 453-12-002 to E.F).

Appendix A

Population receptive field modeling, encoding and model based decoding

A general formulation of pRF modeling is:

$$y_j(t) = \int_0^T \left\{ \sum_{i=1}^{N_r} b_i \left[\int Z(t-\tau, \mathbf{p}) RF_i(\mathbf{p}|\theta) d\mathbf{p} \right]^n \right\} h(\tau) d\tau + \varepsilon_t \quad (1)$$

where y_j represents the time course of voxel j, $Z(t,\mathbf{p})$ is the temporal sequence of stimuli described by the set of (N_p) model parameters $\mathbf{p}$. $Z(t,\mathbf{p})$ is further factorized as the product of a design matrix $\mathbf{D}$ and the stimulus representation $\mathbf{S}$ (i.e. $Z(t, \mathbf{p}) = \mathbf{D}(t, s)\mathbf{S}(s, \mathbf{p})$). RF is the receptive field that is parametrized by the set of parameters θ. For generality, the neuronal population response is assumed to be the weighted combination (b_i) of multiple (N_r) overlapping receptive fields. Finally the neuronal response is convolved with the hemodynamic response $h(t)$ of length T. Parameters are estimated with non-linear optimization techniques with high computational load.

By assuming the shape of hemodynamic response function $h(t)$ or estimating it from the data, the problem in (1) can be reformulated in terms of the deconvolved fMRI responses $r_j(s)$ of every voxel j to stimulus s (i.e. considering $y_j(t) = \int_0^T r_j(s, t-\tau) h(\tau) d\tau$):

$$r_j(s) = \left\{ \sum_{i=1}^{N_r} b_i \left[\int S(s, \mathbf{p}) RF_i(\mathbf{p}|\theta) d\mathbf{p} \right]^{n_{i,j}} \right\} + \varepsilon_s \quad (2)$$

If we assume $RF_i(\mathbf{p}|\theta) = \partial(\mathbf{p} - \mathbf{e}_i)$ where $\mathbf{e}_i$ is the ith element of the standard basis of $\Re^{N_p}$ and the number of receptive fields contributing to the response of a voxel N_r is equal to the number of parameters in the model N_p, the problem in (2) reduces to:

$$r_j(s) = \left\{ \sum_{i=1}^{N_p} b_i [S(s, p_i)]^{n_{i,j}} \right\} + \varepsilon_s \quad (3)$$

Fixing the non linear parameter $n_{i,j}$ for all voxels and receptive fields, and considering it as part of the model representation of the stimuli (i.e. $[S(s, p_i)]^{n_{i,j}} = M(s, p_i)$), a linearized representation of the fMRI response of a voxel as function of the stimulus representation model can be obtained by solving:

$$r_j(s) = \sum_{i=1}^{N_p} b_i M(s, p_i) + \varepsilon_s \quad (4)$$

that can be written also as:

$$\mathbf{r}_j = \mathbf{Mb} + \varepsilon_s \quad (5)$$

where $\mathbf{r}_j$ ($N_s \times 1$) is the vector of responses of voxel j to all N_s stimuli, $\mathbf{M}$ ($N_s \times N_p$) is the model representation of the stimuli and $\mathbf{b}$ ($N_p \times 1$) is a vector representing the contribution of each model parameter to the response. A regularized linear fit (e.g. based on Ridge Regression) can be used to estimate $\mathbf{b}$. The same problem can be formulated on the original time series $y_j(t)$ and not on the deconvolved responses $\mathbf{r}_j$ by convolving the matrix $\mathbf{M}$ with the hemodynamic response $h(t)$.

In model based decoding, the features of the stimulus model based representation are the dependent variables and the fMRI response patterns are the independent variable of a linear regression (Miyawaki et al., 2008). Thus, it can be formulated as:

$$\mathbf{m}_p = \mathbf{Rc} + \varepsilon \quad (6)$$

where $\mathbf{m}_p$ ($N_s \times 1$) is pth feature of the stimulus representation matrix $\mathbf{M}$, $\mathbf{R}$ ($N_s \times N_v$) is the matrix of the fMRI response patterns for all stimuli N_s across all voxels N_v and $\mathbf{c}$ ($N_v \times 1$) is a vector that represents the weighted contribution of each voxel to the decoding of the feature under investigation. As for the model in (5) the problem formulated in (6) can be considered in the original time series domain by considering instead of $\mathbf{m}_p$ its convolution with the hemodynamic response function $h(t)$ and, instead of $\mathbf{R}$ ($N_s \times N_v$), the matrix $\mathbf{Y}$ ($N_t \times N_v$) containing the original fMRI time series of all N_v voxels.

References

Ahveninen, J., Chang, W.T., Huang, S., Keil, B., Kopco, N., Rossi, S., Bonmassar, G., Witzel, T., Polimeni, J.R., 2016. Intracortical depth analyses of frequency-sensitive regions of human auditory cortex using 7TfMRI. Neuroimage 143, 116–127.

Alink, A., Krugliak, A., Walther, A., Kriegeskorte, N., 2013. fMRI orientation decoding in V1 does not require global maps or globally coherent orientation stimuli. Front Psychol. 4, 493.

Anderson, A.J., Zinszer, B.D., Raizada, R.D., 2016. Representational similarity encoding for fMRI: pattern-based synthesis to predict brain activity using stimulus-model-similarities. Neuroimage 128, 44–53.

Andersson, P., Pluim, J.P., Siero, J.C., Klein, S., Viergever, M.A., Ramsey, N.F., 2011. Real-time decoding of brain responses to visuospatial attention using 7T fMRI. PLoS One 6, e27638.

Bandettini, P.A., Wong, E.C., Hinks, R.S., Tikofsky, R.S., Hyde, J.S., 1992. Time course EPI of human brain function during task activation. Magnetic resonance in medicine. Off. J. Soc. Magn. Reson. Med./Soc. Magn. Reson. Med. 25, 390–397.

Barth, M., Norris, D.G., 2007. Very high-resolution three-dimensional functional MRI of the human visual cortex with elimination of large venous vessels. NMR Biomed. 20, 477–484.
Batson, M.A., Petridou, N., Klomp, D.W., Frens, M.A., Neggers, S.F., 2015. Single session imaging of cerebellum at 7 T: obtaining structure and function of multiple motor subsystems in individual subjects. PLoS One 10, e0134933.
Beckett, A., Peirce, J.W., Sanchez-Panchuelo, R.M., Francis, S., Schluppeck, D., 2012. Contribution of large scale biases in decoding of direction-of-motion from high-resolution fMRI data in human early visual cortex. Neuroimage 63, 1623–1632.
Belin, P., Zatorre, R.J., Lafaille, P., Ahad, P., Pike, B., 2000. Voice-selective areas in human auditory cortex. Nature 403, 309–312.
Berron, D., Schutze, H., Maass, A., Cardenas-Blanco, A., Kuijf, H.J., Kumaran, D., Duzel, E., 2016. Strong Evidence for Pattern Separation in Human Dentate Gyrus. J. Neurosci. 36, 7569–7579.
Bianciardi, M., Toschi, N., Eichner, C., Polimeni, J.R., Setsompop, K., Brown, E.N., Hamalainen, M.S., Rosen, B.R., Wald, L.L., 2016. In vivo functional connectome of human brainstem nuclei of the ascending arousal, autonomic, and motor systems by high spatial resolution 7-Tesla fMRI. Magma 29, 451–462.
Bode, S., He, A.H., Soon, C.S., Trampel, R., Turner, R., Haynes, J.D., 2011. Tracking the unconscious generation of free decisions using ultra-high field fMRI. PLoS One 6, e21612.
Boxerman, J.L., Bandettini, P.A., Kwong, K.K., Baker, J.R., Davis, T.L., Rosen, B.R., Weisskoff, R.M., 1995. The intravascular contribution to fMRI signal change: monte Carlo modeling and diffusion-weighted studies in vivo. Magn. Reson. Med. 34, 4–10.
Boyacioglu, R., Schulz, J., Muller, N.C., Koopmans, P.J., Barth, M., Norris, D.G., 2014. Whole brain, high resolution multiband spin-echo EPI fMRI at 7 T: a comparison with gradient-echo EPI using a color-word Stroop task. Neuroimage 97, 142–150.
Budde, J., Shajan, G., Zaitsev, M., Scheffler, K., Pohmann, R., 2014. Functional MRI in human subjects with gradient-echo and spin-echo EPI at 9.4 T. Magn. Reson. Med. 71, 209–218.
Chaimow, D., Yacoub, E., Ugurbil, K., Shmuel, A., 2011. Modeling and analysis of mechanisms underlying fMRI-based decoding of information conveyed in cortical columns. Neuroimage 56, 627–642.
Chen, G., Wang, F., Gore, J.C., Roe, A.W., 2013. Layer-specific BOLD activation in awake monkey V1 revealed by ultra-high spatial resolution functional magnetic resonance imaging. Neuroimage 64, 147–155.
Cox, D.D., Savoy, R.L., 2003. Functional magnetic resonance imaging (fMRI) "brain reading": detecting and classifying distributed patterns of fMRI activity in human visual cortex. Neuroimage 19, 261–270.
Da Costa, S., van der Zwaag, W., Miller, L.M., Clarke, S., Saenz, M., 2013. Tuning in to sound: frequency-selective attentional filter in human primary auditory cortex. J. Neurosci. 33, 1858–1863.
de Haas, B., Schwarzkopf, D.S., Anderson, E.J., Rees, G., 2014. Perceptual load affects spatial tuning of neuronal populations in human early visual cortex. Curr. Biol. 24, R66–R67.
De Martino, F., Esposito, F., Van de Moortele, P.-F., Harel, N., Formisano, E., Goebel, R., Ugurbil, K., Yacoub, E., 2011. Whole brain high-resolution functional imaging at ultra high magnetic fields: an application to the analysis of resting state networks. Neuroimage.
De Martino, F., Moerel, M., Ugurbil, K., Goebel, R., Yacoub, E., Formisano, E., 2015. Frequency preference and attention effects across cortical depths in the human primary auditory cortex. Proc. Natl. Acad. Sci. USA 112, 16036–16041.
De Martino, F., Moerel, M., van de Moortele, P.-F., Ugurbil, K., Goebel, R., Yacoub, E., Formisano, E., 2013a. Spatial organization of frequency preference and selectivity in the human inferior colliculus. Nat. Commun., 4.
De Martino, F., Moerel, M., Xu, J., van de Moortele, P.F., Ugurbil, K., Goebel, R., Yacoub, E., Formisano, E., 2014. High-Resolution Mapping of Myeloarchitecture In Vivo: localization of Auditory Areas in the Human Brain. Cereb. Cortex.
De Martino, F., Valente, G., Staeren, N., Ashburner, J., Goebel, R., Formisano, E., 2008. Combining multivariate voxel selection and support vector machines for mapping and classification of fMRI spatial patterns. Neuroimage 43, 44–58.
De Martino, F., Zimmermann, J., Muckli, L., Ugurbil, K., Yacoub, E., Goebel, R., 2013b. Cortical Depth Dependent Functional Responses in Humans at 7T: improved Specificity with 3D GRASE. PLoS One 8, e60514.
Denison, R.N., Vu, A.T., Yacoub, E., Feinberg, D.A., Silver, M.A., 2014. Functional mapping of the magnocellular and parvocellular subdivisions of human LGN. Neuroimage 102 (Pt 2), 358–369.
Dumoulin, S.O., Fracasso, A., van der Zwaag, W., Siero, J.C., Petridou, N., 2017. Ultra-high field MRI: advancing systems neuroscience towards mesoscopic human brain function. Neuroimage.
Dumoulin, S.O., Wandell, B.A., 2008. Population receptive field estimates in human visual cortex. Neuroimage 39, 647–660.
Ejaz, N., Hamada, M., Diedrichsen, J., 2015. Hand use predicts the structure of representations in sensorimotor cortex. Nat. Neurosci. 18, 1034–1040.
Emmerling, T.C., Zimmermann, J., Sorger, B., Frost, M.A., Goebel, R., 2016. Decoding the direction of imagined visual motion using 7T ultra-high field fMRI. Neuroimage 125, 61–73.
Faull, O.K., Jenkinson, M., Clare, S., Pattinson, K.T., 2015. Functional subdivision of the human periaqueductal grey in respiratory control using 7 T fMRI. Neuroimage 113, 356–364.
FitzPatrick, K.A., 1975. Cellular architecture and topographic organization of the inferior colliculus of the squirrel monkey. J. Comp. Neurol. 164, 185–207.
Formisano, E., De Martino, F., Bonte, M., Goebel, R., 2008. "Who" is saying "what"? Brain-based decoding of human voice and speechScience (New York, NY) 322, 970–973.
Formisano, E., Kim, D.S., Di Salle, F., van De Moortele, P.-F., Ugurbil, K., Goebel, R., 2003. Mirror-symmetric tonotopic maps in human primary auditory cortex. Neuron 40, 859–869.
Fracasso, A., Petridou, N., Dumoulin, S.O., 2014. Distinct BOLD laminar profiles elicited by retino-cortical and inter-hemispheric sources in human early visual cortex. Proc. Int. Soc. Mag. Reson Med. 52, 4435.
Fracasso, A., Petridou, N., Dumoulin, S.O., 2016. Systematic variation of population receptive field properties across cortical depth in human visual cortex. Neuroimage 139, 427–438.
Frahm, J., Merboldt, K.D., Hänicke, W., Kleinschmidt, A., Boecker, H., 1994. Brain or vein–oxygenation or flow? On signal physiology in functional MRI of human brain activation. NMR Biomed. 7, 45–53.
Freeman, J., Brouwer, G.J., Heeger, D.J., Merriam, E.P., 2011. Orientation decoding depends on maps, not columns. J. Neurosci. 31, 4792–4804.
Friston, K., Holmes, A., Worsley, K., Poline, J.-B., Frith, C., Frackowiak, R., 1995. Statistical parametric maps in functional imaging: a general linear approach. Human. Brain Mapp. 2, 11.
Gagnon, L., Sakadzic, S., Lesage, F., Musacchia, J.J., Lefebvre, J., Fang, Q., Yucel, M.A., Evans, K.C., Mandeville, E.T., Cohen-Adad, J., Polimeni, J.R., Yaseen, M.A., Lo, E.H., Greve, D.N., Buxton, R.B., Dale, A.M., Devor, A., Boas, D.A., 2015. Quantifying the microvascular origin of BOLD-fMRI from first principles with two-photon microscopy and an oxygen-sensitive nanoprobe. J. Neurosci. 35, 3663–3675.
Gardumi, A., Ivanov, D., Hausfeld, L., Valente, G., Formisano, E., Uludag, K., 2016. The effect of spatial resolution on decoding accuracy in fMRI multivariate pattern analysis. Neuroimage 132, 32–42.
Gati, J.S., Menon, R.S., Ugurbil, K., Rutt, B.K., 1997. Experimental determination of the BOLD field strength dependence in vessels and tissue. Magn. Reson Med. 38, 296–302.
Geyer, S., Weiss, M., Reimann, K., Lohmann, G., Turner, R., 2011. Microstructural parcellation of the human cerebral cortex - From Brodmann's post-mortem map to in vivo mapping with high-field magnetic resonance imaging. Front. Human. Neurosci. 5, 19.
Glasser, M.F., Coalson, T.S., Robinson, E.C., Hacker, C.D., Harwell, J., Yacoub, E., Ugurbil, K., Andersson, J., Beckmann, C.F., Jenkinson, M., Smith, S.M., Van Essen, D.C., 2016. A multi-modal parcellation of human cerebral cortex. Nature 536, 171–178.
Goense, J., Bohraus, Y., Logothetis, N.K., 2016. fMRI at High Spatial Resolution: implications for BOLD-Models. Front Comput. Neurosci. 10, 66.
Goense, J., Merkle, H., Logothetis, N.K., 2012. High-resolution fMRI reveals laminar differences in neurovascular coupling between positive and negative BOLD responses. Neuron 76, 629–639.
Goense, J.B.M., Logothetis, N.K., 2006. Laminar specificity in monkey V1 using high-resolution SE-fMRI. Magn. Reson. Imaging 24, 381–392.
Goncalves, N.R., Ban, H., Sanchez-Panchuelo, R.M., Francis, S.T., Schluppeck, D., Welchman, A.E., 2015. 7 T FMRI reveals systematic functional organization for binocular disparity in dorsal visual cortex. J. Neurosci. 35, 3056–3072.
Greicius, M.D., Krasnow, B., Reiss, A.L., Menon, V., 2003. Functional connectivity in the resting brain: a network analysis of the default mode hypothesis. Proc. Natl. Acad. Sci. USA 100, 253–258.
Guidi, M., Huber, L., Lampe, L., Gauthier, C.J., Moller, H.E., 2016. Lamina-dependent calibrated BOLD response in human primary motor cortex. Neuroimage 141, 250–261.
Gutteling, T.P., Petridou, N., Dumoulin, S.O., Harvey, B.M., Aarnoutse, E.J., Kenemans, J.L., Neggers, S.F., 2015. Action preparation shapes processing in early visual cortex. J. Neurosci. 35, 6472–6480.
Haak, K.V., Winawer, J., Harvey, B.M., Renken, R., Dumoulin, S.O., Wandell, B.A., Cornelissen, F.W., 2013. Connective field modeling. Neuroimage 66, 376–384.
Hale, J.R., Brookes, M.J., Hall, E.L., Zumer, J.M., Stevenson, C.M., Francis, S.T., Morris, P.G., 2010. Comparison of functional connectivity in default mode and sensorimotor networks at 3 and 7 T. Magma (New Y., NY).
Harvey, B.M., Fracasso, A., Petridou, N., Dumoulin, S.O., 2015. Topographic representations of object size and relationships with numerosity reveal generalized quantity processing in human parietal cortex. Proc. Natl. Acad. Sci. U S A 112, 13525–13530.
Harvey, B.M., Klein, B.P., Petridou, N., Dumoulin, S.O., 2013. Topographic representation of numerosity in the human parietal cortex. Science 341, 1123–1126.
Havlicek, M., Roebroeck, A., Friston, K., Gardumi, A., Ivanov, D., Uludag, K., 2015. Physiologically informed dynamic causal modeling of fMRI data. Neuroimage 122, 355–372.
Haxby, J.V., Gobbini, M.I., Furey, M.L., Ishai, A., Schouten, J.L., Pietrini, P., 2001. Distributed and overlapping representations of faces and objects in ventral temporal cortex. Sci. (New Y., NY) 293, 2425–2430.
Haynes, J.-D., Rees, G., 2005. Predicting the orientation of invisible stimuli from activity in human primary visual cortex. Nat. Neurosci. 8, 686–691.
Heidemann, R.M., Ivanov, D., Trampel, R., Fasano, F., Meyer, H., Pfeuffer, J., Turner, R., 2012. Isotropic submillimeter fMRI in the human brain at 7 T: combining reduced field-of-view imaging and partially parallel acquisitions. Magn. Reson Me.d 68, 1506–1516.
Heinzle, J., Koopmans, P.J., den Ouden, H.E., Raman, S., Stephan, K.E., 2016. A hemodynamic model for layered BOLD signals. Neuroimage 125, 556–570.
Hoffmann, M.B., Stadler, J., Kanowski, M., Speck, O., 2009. Retinotopic mapping of the human visual cortex at a magnetic field strength of 7T. Clinical neurophysiology. Off. J. Int. Fed. Clin. Neurophysiol. 120, 108–116.
Hua, J., Qin, Q., van Zijl, P.C., Pekar, J.J., Jones, C.K., 2014. Whole-brain three-dimensional T2-weighted BOLD functional magnetic resonance imaging at 7 T.

Magn. Reson. Med. 72, 1530–1540.
Hubel, D.H., Wiesel, T.N., 1968. Receptive fields and functional architecture of monkey striate cortex. J. Physiol. 195, 215–243.
Huber, L., Goense, J., Kennerley, A.J., Trampel, R., Guidi, M., Reimer, E., Ivanov, D., Neef, N., Gauthier, C.J., Turner, R., Moller, H.E., 2015. Cortical lamina-dependent blood volume changes in human brain at 7 T. Neuroimage 107, 23–33.
Huber, L., Ivanov, D., Guidi, M., Turner, R., Uludag, K., Moller, H.E., Poser, B.A., 2016. Functional cerebral blood volume mapping with simultaneous multi-slice acquisition. Neuroimage 125, 1159–1168.
Hutton, C., Josephs, O., Stadler, J., Featherstone, E., Reid, A., Speck, O., Bernarding, J., Weiskopf, N., 2011. The impact of physiological noise correction on fMRI at 7T. Neuroimage, 1–48.
Kajikawa, Y., Schroeder, C.E., 2011. How local is the local field potential? Neuron 72, 847–858.
Kajikawa, Y., Schroeder, C.E., 2015. Generation of field potentials and modulation of their dynamics through volume integration of cortical activity. J. Neurophysiol. 113, 339–351.
Kamitani, Y., Tong, F., 2005. Decoding the visual and subjective contents of the human brain. Nat. Neurosci. 8, 679–685.
Kanwisher, N., McDermott, J., Chun, M.M., 1997. The fusiform face area: a module in human extrastriate cortex specialized for face perception. J. Neurosci. 17, 4302–4311.
Kay, K.N., Naselaris, T., Prenger, R.J., Gallant, J.L., 2008. Identifying natural images from human brain activity. Nature 452, 352–355.
Kay, K.N., Weiner, K.S., Grill-Spector, K., 2015. Attention reduces spatial uncertainty in human ventral temporal cortex. Curr. Biol. 25, 595–600.
Kay, K.N., Winawer, J., Mezer, A., Wandell, B.A., 2013a. Compressive spatial summation in human visual cortex. J Neurophysiol. 110, 481–494.
Kay, K.N., Winawer, J., Rokem, A., Mezer, A., Wandell, B.A., 2013b. A two-stage cascade model of BOLD responses in human visual cortex. PLoS Comput. Biol. 9, e1003079.
Kemper, V.G., De Martino, F., Emmerling, T.C., Yacoub, E., Goebel, R., 2017. High resolution data analysis strategies for mesoscale human functional MRI at 7 and9.4 T. under review.
Kemper, V.G., De Martino, F., Vu, A.T., Poser, B.A., Feinberg, D.A., Goebel, R., Yacoub, E., 2015. Sub-millimeter T2 weighted fMRI at 7 T: comparison of 3D-GRASE and 2D SE-EPI. Front. Neurosci. 9, 163.
Kemper, V.G., De Martino, F., Yacoub, E., Goebel, R., 2016. Variable flip angle 3D-GRASE for high resolution fMRI at 7 T. Magn. Reson. Med. 76, 897–904.
Keuken, M.C., Van Maanen, L., Bogacz, R., Schafer, A., Neumann, J., Turner, R., Forstmann, B.U., 2015. The subthalamic nucleus during decision-making with multiple alternatives. Hum. Brain Mapp. 36, 4041–4052.
Klein, B.P., Harvey, B.M., Dumoulin, S.O., 2014. Attraction of position preference by spatial attention throughout human visual cortex. Neuron 84, 227–237.
Kok, P., Bains, L.J., van Mourik, T., Norris, D.G., de Lange, F.P., 2016. Selective Activation of the Deep Layers of the Human Primary Visual Cortex by Top-Down Feedback. Curr. Biol. 26, 371–376.
Koopmans, P.J., Barth, M., Norris, D.G., 2010. Layer-specific BOLD activation in human V1. Human. Brain Mapp. 31, 1297–1304.
Koopmans, P.J., Barth, M., Orzada, S., Norris, D.G., 2011. Multi-echo fMRI of the cortical laminae in humans at 7T. Neuroimage 56, 1276–1285.
Koopmans, P.J., Boyacioglu, R., Barth, M., Norris, D.G., 2012. Whole brain, high resolution spin-echo resting state fMRI using PINS multiplexing at 7 T. Neuroimage 62, 1939–1946.
Krebs, R.M., Woldorff, M.G., Tempelmann, C., Bodammer, N., Noesselt, T., Boehler, C.N., Scheich, H., Hopf, J.-M., Duzel, E., Heinze, H.-J., Schoenfeld, M.A., 2010. High-field FMRI reveals brain activation patterns underlying saccade execution in the human superior colliculus. PLoS One 5, e8691.
Kriegeskorte, N., Cusack, R., Bandettini, P., 2010. How does an fMRI voxel sample the neuronal activity pattern: compact-kernel or complex spatiotemporal filter? Neuroimage 49, 1965–1976.
Kriegeskorte, N., Goebel, R., Bandettini, P., 2006. Information-based functional brain mapping. Proc. Natl. Acad. Sci. USA 103, 3863–3868.
Kriegeskorte, N., Mur, M., Bandettini, P.A., 2008. Representational similarity analysis - connecting the branches of systems neuroscience. Front. Syst. Neurosci. 2, 4.
Kuehn, E., Trampel, R., Mueller, K., Turner, R., Schutz-Bosbach, S., 2013. Judging roughness by sight–a 7-Tesla fMRI study on responsivity of the primary somatosensory cortex during observed touch of self and others. Hum. Brain Mapp. 34, 1882–1895.
Kuper, M., Thurling, M., Stefanescu, R., Maderwald, S., Roths, J., Elles, H.G., Ladd, M.E., Diedrichsen, J., Timmann, D., 2012. Evidence for a motor somatotopy in the cerebellar dentate nucleus–an FMRI study in humans. Hum. Brain Mapp. 33, 2741–2749.
Kwong, K.K., Belliveau, J.W., Chesler, D.A., Goldberg, I.E., Weisskoff, R.M., Poncelet, B.P., Kennedy, D.N., Hoppel, B.E., Cohen, M.S., Turner, R., 1992. Dynamic magnetic resonance imaging of human brain activity during primary sensory stimulation. Proc. Natl. Acad. Sci. USA 89, 5675–5679.
Lai, S., Hopkins, A.L., Haacke, E.M., Li, D., Wasserman, B.A., Buckley, P., Friedman, L., Meltzer, H., Hedera, P., Friedland, R., 1993. Identification of vascular structures as a major source of signal contrast in high resolution 2D and 3D functional activation imaging of the motor cortex at 1.5T: preliminary results. Magnetic resonance in medicine. Off. J. Soc. Magn. Reson. Med./Soc. Magn. Reson. Med. 30, 387–392.
Lenglet, C., Abosch, A., Yacoub, E., De Martino, F., Sapiro, G., Harel, N., 2012. Comprehensive in vivo mapping of the human basal ganglia and thalamic connectome in individuals using 7T MRI. PLoS One 7, e29153.
Logothetis, N.K., 2008. What we can do and what we cannot do with fMRI. Nature 453, 869–878.
Logothetis, N.K., Pauls, J., Augath, M., Trinath, T., Oeltermann, A., 2001. Neurophysiological investigation of the basis of the fMRI signal. Nature 412, 150–157.
Lu, H., Golay, X., Pekar, J.J., Van Zijl, P.C., 2003. Functional magnetic resonance imaging based on changes in vascular space occupancy. Magn. Reson. Med. 50, 263–274.
Lu, H., van Zijl, P.C., 2012. A review of the development of Vascular-Space-Occupancy (VASO) fMRI. Neuroimage 62, 736–742.
Maass, A., Berron, D., Libby, L.A., Ranganath, C., Duzel, E., 2015. Functional subregions of the human entorhinal cortex. Elife, 4.
Maass, A., Schutze, H., Speck, O., Yonelinas, A., Tempelmann, C., Heinze, H.J., Berron, D., Cardenas-Blanco, A., Brodersen, K.H., Stephan, K.E., Duzel, E., 2014. Laminar activity in the hippocampus and entorhinal cortex related to novelty and episodic encoding. Nat. Commun. 5, 5547.
Mansfield, P., 1977. Multi-planar image formation using NMR spin echoes. J. Phys. C: Solid State Phys.
Markuerkiaga, I., Barth, M., Norris, D.G., 2016. A cortical vascular model for examining the specificity of the laminar BOLD signal. Neuroimage 132, 491–498.
Martuzzi, R., van der Zwaag, W., Farthouat, J., Gruetter, R., Blanke, O., 2014. Human finger somatotopy in areas 3b, 1, and 2: a 7T fMRI study using a natural stimulus. Hum. Brain Mapp. 35, 213–226.
Merzenich, M.M., Reid, M.D., 1974. Representation of the cochlea within the inferior colliculus of the cat. Brain Res. 77, 397–415.
Mestres-Misse, A., Trampel, R., Turner, R., Kotz, S.A., 2016. Uncertainty and expectancy deviations require cortico-subcortical cooperation. Neuroimage.
Mestres-Misse, A., Turner, R., Friederici, A.D., 2012. An anterior-posterior gradient of cognitive control within the dorsomedial striatum. Neuroimage 62, 41–47.
Metzger, C.D., Eckert, U., Steiner, J., Sartorius, A., Buchmann, J.E., Stadler, J., Tempelmann, C., Speck, O., Bogerts, B., Abler, B., Walter, M., 2010. High field FMRI reveals thalamocortical integration of segregated cognitive and emotional processing in mediodorsal and intralaminar thalamic nuclei. Front Neuroanat. 4, 138.
Mitra, P.P., 2014. The circuit architecture of whole brains at the mesoscopic scale. Neuron 83, 1273–1283.
Miyawaki, Y., Uchida, H., Yamashita, O., Sato, M.-a, Morito, Y., Tanabe, H.C., Sadato, N., Kamitani, Y., 2008. Visual image reconstruction from human brain activity using a combination of multiscale local image decoders. Neuron 60, 915–929.
Moeller, S., Yacoub, E., Olman, C.A., Auerbach, E.J., Strupp, J.P., Harel, N., Ugurbil, K., 2010. Multiband multislice GE-EPI at 7 T, with 16-fold acceleration using partial parallel imaging with application to high spatial and temporal whole-brain fMRI. Magn. Reson. Med. 63, 1144–1153.
Moerel, M., De Martino, F., Formisano, E., 2012. Processing of natural sounds in human auditory cortex: tonotopy, spectral tuning and relation to voice-sensitivity. J. Neurosci. 32, 14205–14216.
Moerel, M., De Martino, F., Santoro, R., Ugurbil, K., Goebel, R., Yacoub, E., Formisano, E., 2013. Processing of natural sounds: characterization of multipeak spectral tuning in human auditory cortex. J Neurosci. 33, 11888–11898.
Moerel, M., De Martino, F., Santoro, R., Yacoub, E., Formisano, E., 2015a. Representation of pitch chroma by multi-peak spectral tuning in human auditory cortex. Neuroimage 106, 161–169.
Moerel, M., De Martino, F., Ugurbil, K., Yacoub, E., Formisano, E., 2015b. Processing of frequency and location in human subcortical auditory structures. Sci. Rep. 5, 17048.
Mountcastle, V.B., 1997. The columnar organization of the neocortex. Brain 120 (Pt 4), 701–722.
Mourao-Miranda, J., Bokde, A., Born, C., Hampel, H., 2005. Classifying brain states and determining the discriminating activation patterns: support vector machine on functional MRI data. Neuroimage.
Muckli, L., De Martino, F., Vizioli, L., Petro, L.S., Smith, F.W., Ugurbil, K., Goebel, R., Yacoub, E., 2015. Contextual Feedback to Superficial Layers of V1. Curr. Biol. 25, 2690–2695.
Naselaris, T., Kay, K.N., 2015. Resolving Ambiguities of MVPA Using Explicit Models of Representation. Trends Cogn. Sci. 19, 551–554.
Naselaris, T., Kay, K.N., Nishimoto, S., Gallant, J.L., 2010. Encoding and decoding in fMRI. Neuroimage.
Nasr, S., Polimeni, J.R., Tootell, R.B., 2016. Interdigitated Color- and Disparity-Selective Columns within Human Visual Cortical Areas V2 and V3. J. Neurosci. 36, 1841–1857.
Nili, H., Wingfield, C., Walther, A., Su, L., Marslen-Wilson, W., Kriegeskorte, N., 2014. A toolbox for representational similarity analysis. PLoS Comput. Biol. 10, e1003553.
O'Herron, P., Chhatbar, P.Y., Levy, M., Shen, Z., Schramm, A.E., Lu, Z., Kara, P., 2016. Neural correlates of single-vessel haemodynamic responses in vivo. Nature 534, 378–382.
Ogawa, S., Lee, T.M., Kay, A.R., Tank, D.W., 1990. Brain magnetic resonance imaging with contrast dependent on blood oxygenation. Proc. Natl. Acad. Sci. USA 87, 9868–9872.
Ogawa, S., Tank, D.W., Menon, R.S., Ellermann, J.M., Kim, S.-G., Merkle, H., Ugurbil, K., 1992. Intrinsic signal changes accompanying sensory stimulation: functional brain mapping with magnetic resonance imaging. PNAS (USA) 89, 5951–5955.
Olman, C., Harel, N., Feinberg, D.A., He, S., Zhang, P., Ugurbil, K., Yacoub, E., 2012. Layer-Specific fMRI reflect different nuronal computations at different depths in human V1. PLoS One 7, e32536, (doi:32510.31371/journal.pone.0032536).
Olman, C.A., Van de Moortele, P.-F., Yacoub, E., 2010. Retinotopic mapping with spin echo BOLD at 7T. Magn. Reson. Imaging 6.
Op de Beeck, H.P., 2010a. Against hyperacuity in brain reading: spatial smoothing does not hurt multivariate fMRI analyses? Neuroimage 49, 1943–1948.
Op de Beeck, H.P., 2010b. Probing the mysterious underpinnings of multi-voxel fMRI analyses. Neuroimage 50, 567–571.

Oshio, K., Feinberg, D.A., 1991. GRASE (Gradient- and spin-echo) imaging: a novel fast MRI technique. Magn. Reson Med 20, 344–349.
Peer, M., Salomon, R., Goldberg, I., Blanke, O., Arzy, S., 2015. Brain system for mental orientation in space, time, and person. Proc. Natl. Acad. Sci. USA 112, 11072–11077.
Pereira, F., Mitchell, T.M., Botvinick, M., 2009. Machine learning classifiers and fMRI: a tutorial overview. Neuroimage 45, S199–S209.
Pohmann, R., Speck, O., Scheffler, K., 2016. Signal-to-noise ratio and MR tissue parameters in human brain imaging at 3, 7, and 9.4 T using current receive coil arrays. Magn. Reson. Med. 75, 801–809.
Polimeni, J.R., Fischl, B., Greve, D.N., Wald, L.L., 2010. Laminar analysis of 7T BOLD using an imposed spatial activation pattern in human V1. Neuroimage 52, 1334–1346.
Renvall, V., Witzel, T., Wald, L.L., Polimeni, J.R., 2016. Automatic cortical surface reconstruction of high-resolution T1 echo planar imaging data. Neuroimage 134, 338–354.
Ress, D., Glover, G.H., Liu, J., Wandell, B., 2007. Laminar profiles of functional activity in the human brain. Neuroimage 34, 74–84.
Roberts, M.J., Lowet, E., Brunet, N.M., Ter Wal, M., Tiesinga, P., Fries, P., De Weerd, P., 2013. Robust gamma coherence between macaque V1 and V2 by dynamic frequency matching. Neuron 78, 523–536.
Sanchez Panchuelo, R.M., Ackerley, R., Glover, P.M., Bowtell, R.W., Wessberg, J., Francis, S.T., McGlone, F., 2016. Mapping quantal touch using 7 T functional magnetic resonance imaging and single-unit intraneural microstimulation. Elife, 5.
Sanchez-Panchuelo, R.M., Besle, J., Beckett, A., Bowtell, R., Schluppeck, D., Francis, S., 2012a. Within-digit functional parcellation of Brodmann areas of the human primary somatosensory cortex using functional magnetic resonance imaging at 7 T. J. Neurosci. 32, 15815–15822.
Sanchez-Panchuelo, R.M., Besle, J., Mougin, O., Gowland, P., Bowtell, R., Schluppeck, D., Francis, S., 2014. Regional structural differences across functionally parcellated Brodmann areas of human primary somatosensory cortex. Neuroimage 93 (Pt 2), 221–230.
Sanchez-Panchuelo, R.M., Francis, S.T., Bowtell, R., Schluppeck, D., 2010. Mapping human somatosensory cortex in individual subjects with 7T functional MRI. J. Neurophysiol. 103, 2544–2556.
Sanchez-Panchuelo, R.M., Francis, S.T., Schluppeck, D., Bowtell, R.W., 2012b. Correspondence of human visual areas identified using functional and anatomical MRI in vivo at 7 T. J Magn. Reson Imaging 35, 287–299.
Santoro, R., Moerel, M., De Martino, F., Goebel, R., Ugurbil, K., Yacoub, E., Formisano, E., 2014. Encoding of natural sounds at multiple spectral and temporal resolutions in the human auditory cortex. PLoS Comput. Biol. 10, e1003412.
Santoro, R., Moerel, M., De Martino, F., Ugurbil, K., Yacoub, E., Formisano, E., 2012. Representation of natural sounds in the human auditory cortex. Proc. Soc. Neurosci., (2012).
Sasaki, Y., Rajimehr, R., Kim, B.W., Ekstrom, L.B., Vanduffel, W., Tootell, R.B., 2006. The radial bias: a different slant on visual orientation sensitivity in human and nonhuman primates. Neuron 51, 661–670.
Schallmo, M.P., Grant, A.N., Burton, P.C., Olman, C.A., 2016. The effects of orientation and attention during surround suppression of small image features: a 7 T fMRI study. J. Vis. 16, 19.
Scheeringa, R., Koopmans, P.J., van Mourik, T., Jensen, O., Norris, D.G., 2016. The relationship between oscillatory EEG activity and the laminar-specific BOLD signal. Proc. Natl. Acad. Sci. USA 113, 6761–6766.
Scheffler, K., Ehses, P., 2016. High-resolution mapping of neuronal activation with balanced SSFP at 9.4 T. Magn. Reson. Med. 76, 163–171.
Schellekens, W., van Wezel, R.J., Petridou, N., Ramsey, N.F., Raemaekers, M., 2016. Predictive coding for motion stimuli in human early visual cortex. Brain Struct. Funct. 221, 879–890.
Sereno, M.I., Dale, A.M., Reppas, J.B., Kwong, K.K., Belliveau, J.W., Brady, T.J., Rosen, B.R., Tootell, R.B., 1995. Borders of multiple visual areas in humans revealed by functional magnetic resonance imaging. Science 268, 889–893.
Setsompop, K., Gagoski, B.A., Polimeni, J.R., Witzel, T., Wedeen, V.J., Wald, L.L., 2012. Blipped-controlled aliasing in parallel imaging for simultaneous multislice echo planar imaging with reduced g-factor penalty. Magn. Reson Med 67, 1210–1224.
Shmuel, A., Yacoub, E., Chaimow, D., Logothetis, N.K., Ugurbil, K., 2007. Spatio-temporal point-spread function of fMRI signal in human gray matter at 7 T. Neuroimage 35, 539–552.
Siero, J.C., Hermes, D., Hoogduin, H., Luijten, P.R., Ramsey, N.F., Petridou, N., 2014. BOLD matches neuronal activity at the mm scale: a combined 7T fMRI and ECoG study in human sensorimotor cortex. Neuroimage 101, 177–184.
Siero, J.C.W., Petridou, N., Hoogduin, H., Luijten, P.R., Ramsey, N.F., 2011. Cortical depth-dependent temporal dynamics of the BOLD response in the human brain. J Cereb. Blood Flow. Metab. 31, 1999–2008.
Sladky, R., Baldinger, P., Kranz, G.S., Trostl, J., Hoflich, A., Lanzenberger, R., Moser, E., Windischberger, C., 2013. High-resolution functional MRI of the human amygdala at 7 T. Eur. J. Radiol. 82, 728–733.
Sprague, T.C., Serences, J.T., 2013. Attention modulates spatial priority maps in the human occipital, parietal and frontal cortices. Nat. Neurosci. 16, 1879–1887.
Staeren, N., Renvall, H., De Martino, F., Goebel, R., Formisano, E., 2009. Sound categories are represented as distributed patterns in the human auditory cortex. Curr. Biol. 19, 498–502.
Stefanescu, M.R., Thurling, M., Maderwald, S., Wiestler, T., Ladd, M.E., Diedrichsen, J., Timmann, D., 2013. A 7T fMRI study of cerebellar activation in sequential finger movement tasks. Exp. Brain Res. 228, 243–254.
Stelzer, J., Buschmann, T., Lohmann, G., Margulies, D.S., Trampel, R., Turner, R., 2014. Prioritizing spatial accuracy in high-resolution fMRI data using multivariate feature weight mapping. Front Neurosci. 8, 66.
Stringer, E.A., Chen, L.M., Friedman, R.M., Gatenby, J.C., Gore, J.C., 2010. Differentiation of somatosensory cortices by high-resolution fMRI at 7T. Neuroimage.
Suthana, N.A., Donix, M., Wozny, D.R., Bazih, A., Jones, M., Heidemann, R.M., Trampel, R., Ekstrom, A.D., Scharf, M., Knowlton, B., Turner, R., Bookheimer, S.Y., 2015. High-resolution 7T fMRI of human hippocampal subfields during associative learningJ. Cogn. Neurosci. 27, 1194–1206.
Swisher, J.D., Gatenby, J.C., Gore, J.C., Wolfe, B.A., Moon, C.-H., Kim, S.-G., Tong, F., 2010. Multiscale pattern analysis of orientation-selective activity in the primary visual cortex. J. Neurosci. 30, 325–330.
Ten Oever, S., Hausfeld, L., Correia, J.M., Van Atteveldt, N., Formisano, E., Sack, A.T., 2016. A 7T fMRI study investigating the influence of oscillatory phase on syllable representations. Neuroimage 141, 1–9.
Thomas, J.M., Huber, E., Stecker, G.C., Boynton, G.M., Saenz, M., Fine, I., 2015. Population receptive field estimates of human auditory cortex. Neuroimage 105, 428–439.
Torrisi, S., O'Connell, K., Davis, A., Reynolds, R., Balderston, N., Fudge, J.L., Grillon, C., Ernst, M., 2015. Resting state connectivity of the bed nucleus of the stria terminalis at ultra-high field. Hum. Brain Mapp. 36, 4076–4088.
Triantafyllou, C., Hoge, R.D., Krueger, G., Wiggins, C.J., Potthast, A., Wiggins, G.C., Wald, L.L., 2005. Comparison of physiological noise at 1.5 T, 3 T and 7 T and optimization of fMRI acquisition parameters. Neuroimage 26, 243–250.
Turner, R., 2002. How much cortex can a vein drain? Downstream dilution of activation-related cerebral blood oxygenation changes. Neuroimage 16, 1062–1067.
Turner, R., 2016. Uses, misuses, new uses and fundamental limitations of magnetic resonance imaging in cognitive science. Philos. Trans. R Soc. Lond. B Biol. Sci., 371.
Ugurbil, K., 2016. What is feasible with imaging human brain function and connectivity using functional magnetic resonance imaging. Philos. Trans. R Soc. Lond. B Biol. Sci., 371.
Ugurbil, K., Adriany, G., Andersen, P., Chen, W., Garwood, M., Gruetter, R., Henry, P.-G., Kim, S.-G., Lieu, H., Tkac, I., Vaughan, J.T., van De Moortele, P.-F., Yacoub, E., Zhu, X.-H., 2003. Ultrahigh field magnetic resonance imaging and spectroscopy. Magn. Reson. Imaging 21, 1263–1281.
Uğurbil, K., Toth, L., Kim, D.S., 2003. How accurate is magnetic resonance imaging of brain function? Trends Neurosci. 26, 108–114.
Ugurbil, K., Xu, J., Auerbach, E.J., Moeller, S., Vu, A.T., Duarte-Carvajalino, J.M., Lenglet, C., Wu, X., Schmitter, S., Van de Moortele, P.F., Strupp, J., Sapiro, G., De Martino, F., Wang, D., Harel, N., Garwood, M., Chen, L., Feinberg, D.A., Smith, S.M., Miller, K.L., Sotiropoulos, S.N., Jbabdi, S., Andersson, J.L., Glasser, Behrens, T.E., Van Essen, M.F., Yacoub, D.C., Consortium, E., W.U.-M.H, 2013. Pushing spatial and temporal resolution for functional and diffusion MRI in the human connectome project. Neuroimage 80, 80–104.
Uludag, K., Binder, P., 2017. Linking brain vascular physiology to hemodynamic response at ultra-high field MRI. Neuromage.
Uludag, K., Muller-Bierl, B., Ugurbil, K., 2009. An integrative model for neuronal activity-induced signal changes for gradient and spin echo functional imaging. Neuroimage 48, 150–165.
van der Zwaag, W., Da Costa, S.E., Zurcher, N.R., Adams, R.B., Jr, Hadjikhani, N., 2012. A 7 T FMRI study of amygdala responses to fearful faces. Brain Topogr. 25, 125–128.
van der Zwaag, W., Gentile, G., Gruetter, R., Spierer, L., Clarke, S., 2010. Where sound position influences sound object representations: a 7-T fMRI study. Neuroimage.
van der Zwaag, W., Gruetter, R., Martuzzi, R., 2015. Stroking or buzzing? A comparison of somatosensory touch stimuli using 7 T fMRI. PLoS ONE 10, e0134610.
van der Zwaag, W., Kusters, R., Magill, A., Gruetter, R., Martuzzi, R., Blanke, O., Marques, J.P., 2013. Digit somatotopy in the human cerebellum: a 7T fMRI study. Neuroimage 67, 354–362.
van der Zwaag, W., Schafer, A., Marques, J.P., Turner, R., Trampel, R., 2016. Recent applications of UHF-MRI in the study of human brain function and structure: a review. NMR Biomed. 29, 1274–1288.
Vaughan, J.T., Garwood, M., Collins, C.M., Liu, W., DelaBarre, L., Adriany, G., Andersen, P., Merkle, H., Goebel, R., Smith, M.B., Ugurbil, K., 2001. 7T vs. 4T: rf power, homogeneity, and signal-to-noise comparison in head images. Magn. Reson. Med. 46, 24–30.
Vu, A.T., Jamison, K., Glasser, M.F., Smith, S.M., Coalson, T., Moeller, S., Auerbach, E.J., Ugurbil, K., Yacoub, E., 2016a. Tradeoffs in pushing the spatial resolution of fMRI for the 7T human connectome project. Neuroimage.
Vu, A.T., Phillips, J.S., Kay, K., Phillips, M.E., Johnson, M.R., Shinkareva, S.V., Tubridy, S., Millin, R., Grossman, M., Gureckis, T., Bhattacharyya, R., Yacoub, E., 2016b. Using precise word timing information improves decoding accuracy in a multiband-accelerated multimodal reading experiment. Cogn. Neuropsychol. 33, 265–275.
Wacker, E., Spitzer, B., Lutzkendorf, R., Bernarding, J., Blankenburg, F., 2011. Tactile motion and pattern processing assessed with high-field FMRI. PLoS One 6, e24860.
Waehnert, M.D., Dinse, J., Weiss, M., Streicher, M.N., Waehnert, P., Geyer, S., Turner, R., Bazin, P.L., 2014. Anatomically motivated modeling of cortical laminae. Neuroimage 93 (Pt 2), 210–220.
Walter, M., Stadler, J., Tempelmann, C., Speck, O., Northoff, G., 2008. High resolution fMRI of subcortical regions during visual erotic stimulation at 7 T. MAGMA 21, 103–111.
Wandell, B.A., 1999. Computational neuroimaging of human visual cortex. Annu Rev. Neurosci. 22, 145–173.
Wandell, B.A., Winawer, J., 2015. Computational neuroimaging and population receptive fields. Trends Cogn. Sci. 19, 349–357.
Warren, S.G., Yacoub, E., Ghose, G.M., 2014. Featural and temporal attention selectively enhance task-appropriate representations in human primary visual cortex. Nat.

Commun. 5, 5643.
Winer, J.A., Schreiner, C., 2005. The inferior colliculus. Springer Verlag.
Xie, J., Padoa-Schioppa, C., 2016. Neuronal remapping and circuit persistence in economic decisions. Nat. Neurosci. 19, 855–861.
Xu, J., Moeller, S., Auerbach, E.J., Strupp, J., Smith, S.M., Feinberg, D.A., Yacoub, E., Ugurbil, K., 2013. Evaluation of slice accelerations using multiband echo planar imaging at 3T. Neuroimage 83, 991–1001.
y Cajal, S.R., 1995. Histology of the nervous system of man and vertebrates. Oxford University Press, USA.
Yacoub, E., Duong, T.Q., van De Moortele, P.-F., Lindquist, M., Adriany, G., Kim, S.-G., Ugurbil, K., Hu, X., 2003. Spin-echo fMRI in humans using high spatial resolutions and high magnetic fields. Magn. Reson. Med. 49, 655–664.
Yacoub, E., Harel, N., Ugurbil, K., 2008. High-field fMRI unveils orientation columns in humans. PNAS (USA) 105, 10607–10612.
Yacoub, E., Shmuel, A., Logothetis, N., Ugurbil, K., 2007. Robust detection of ocular dominance columns in humans using Hahn Spin Echo BOLD functional MRI at 7 T. Neuroimage 37, 1161–1177.
Yacoub, E., van De Moortele, P.-F., Shmuel, A., Ugurbil, K., 2005. Signal and noise characteristics of Hahn SE and GE BOLD fMRI at 7 T in humans. Neuroimage 24, 738–750.
Yu, X., Glen, D., Wang, S., Dodd, S., Hirano, Y., Saad, Z., Reynolds, R., Silva, A.C., Koretsky, A.P., 2012. Direct imaging of macrovascular and microvascular contributions to BOLD fMRI in layers IV-V of the rat whisker-barrel cortex. Neuroimage 59, 1451–1460.
Zhao, F., Wang, P., Hendrich, K., Kim, S.G., 2005. Spatial specificity of cerebral blood volume-weighted fMRI responses at columnar resolution. Neuroimage 27, 416–424.
Zhao, F., Wang, P., Hendrich, K., Ugurbil, K., Kim, S.-G., 2006. Cortical layer-dependent BOLD and CBV responses measured by spin-echo and gradient-echo fMRI: insights into hemodynamic regulation. Neuroimage 30, 1149–1160.
Zimmermann, J., Goebel, R., De Martino, F., Van de Moortele, P.-F., Feinberg, D., Adriany, G., Chaimow, D., Shmuel, A., Ugurbil, K., Yacoub, E., 2011. Mapping the organization of axis of motion selective features in human area MT using high-field fMRI. PLoS One 6, e28716.